T cell receptor sequencing reveals the distinct development of fetal and adult human Vγ9Vδ2 T cells

Maria Papadopoulou[1,2], Paola Tieppo[1,2], Naomi McGovern[3], Françoise Gosselin[4], Jerry K.Y. Chan[5,6,7], Glenn Goetgeluk[8], Nicolas Dauby[2,9], Alexandra Cogan[10], Catherine Donner[4], Florent Ginhoux[11], Bart Vandekerckhove[8], David Vermijlen[1,2,*]

[1] Department of Pharmacotherapy and Pharmaceutics, Université Libre de Bruxelles (ULB), Bruxelles, Belgium

[2] Institute for Medical Immunology, Université Libre de Bruxelles (ULB), Gosselies, Belgium

[3] Department of Pathology and Centre for Trophoblast Research, University of Cambridge, Cambridge, UK

[4] Department of Obstetrics and Gynecology, Hôpital Erasme, Université Libre de Bruxelles (ULB), Bruxelles, Belgium

[5] Department of Reproductive Medicine, KK Women's and Children's Hospital, Singapore 229899

[6] Department of Obstetrics & Gynaecology, Yong Loo Lin School of Medicine, National University of Singapore, Singapore 119228

[7] OBGYN-Academic Clinical Program, Duke-NUS, Duke-NUS Medical School, Singapore 169857

[8] Department of Clinical chemistry, microbiology and immunology, Ghent University, Ghent, Belgium

[9] Department of Infectious Diseases, Centre Hospitalier Universitaire Saint-Pierre, Université Libre de Bruxelles (ULB), Bruxelles, Belgium

[10] Department of Obstetrics and Gynecology, Centre Hospitalier Universitaire Saint-Pierre, Université Libre de Bruxelles (ULB), Bruxelles, Belgium

[11] Singapore Immunology Network (SIgN), A*STAR, Singapore 138648

*Correspondence to: dvermijl@ulb.ac.be (DV)

Keywords: gammadelta, thymocyte, γδ T cells, human immunology, innate immunity, immunotherapy

Running title: Distinct development of fetal and adult Vγ9Vδ2 T cells

This work was supported by the FNRS (Télévie 7.4555.14, J.0078.13), MP is supported by the FNRS (FRIA), PT is supported by the FNRS (Télévie) and the 'Fondation Rose et Jean Hoguet' and ND is a post-doctoral research fellow of the FNRS. This article is published with the support of the Fondation Universitaire of Belgium.

36 Abbreviations used in this article: BTN3A1, butyrophilin 3A1; CDR3, complementarity-determining-
37 region-3; DETCs, dendritic epidermal T cells; HMBPP, (E)-4-hydroxy-3-methyl-but-2-enyl
38 pyrophosphate; HSPC, hematopoietic-stem-and-precursor-cell; HTS, high-throughput sequencing;
39 IPP, isopentenyl pyrophosphate; MAIT, mucosal-associated invariant T; MEP, 2-C-methyl-D-erythritol
40 4-phosphate; TCR, T cell receptor; TdT, terminal deoxynucleotidyl transferase.

41

Abstract

Phosphoantigen-reactive Vγ9Vδ2 T cells represent the main innate human γδ T cell subset and dominate the fetal and adult peripheral blood γδ T cell repertoire. It has been hypothesized that adult blood Vγ9Vδ2 T cells find their origin in the fetus like it is established for mouse innate γδ T cells. In order to address this issue, we analyzed the complementarity-determining-region-3 (CDR3) of the T cell receptor (TCR) of human blood and thymic Vγ9Vδ2 T cells from fetal until adult life. We first identified key differences in the CDR3 repertoire of fetal and adult blood Vγ9Vδ2 T cells, including in CDR3 features important for phosphoantigen-reactivity. Next, we showed that most of these key adult CDR3 features were already present in the postnatal thymus and were further enhanced upon selection *in vitro* by the microbial-derived phosphoantigen (E)-4-hydroxy-3-methyl-but-2-enyl pyrophosphate (HMBPP). Finally, we demonstrated that the generation of a fetal-type or adult-type Vγ9Vδ2 CDR3 repertoire is determined by the fetal and post-natal nature of the hematopoietic-stem-and-precursor-cell (HSPC). Thus, our data indicate that fetal blood Vγ9Vδ2 T cells find their origin in the fetal thymus while adult blood Vγ9Vδ2 T cells are generated to a large degree independently after birth.

Key points:

- Fetal and adult blood Vγ9Vδ2 T cells express a different CDR3 repertoire
- The post-natal thymus produces a small number of Vγ9Vδ2 thymocytes
- Adult blood Vγ9Vδ2 T cells are derived from postnatal Vγ9Vδ2 thymocytes

Introduction

Since the emergence of jawed vertebrates more than 450 million years ago, γδ T cells have been conserved, and can play an important role in anti-microbial and anti-tumor immunity(1–4). γδ T cells, like αβ T cells and B cells, use V(D)J gene rearrangement with the potential to generate a set of highly diverse receptors to recognize antigens. This diversity is generated mainly in the complementary-determining region 3 (CDR3) of the T cell receptor (TCR) via combinatorial and junctional diversity (5, 6). The junctional diversity is generated during the V(D)J gene segment joining process by: (i) asymmetrical opening of the hairpinned coding ends allowing incorporation of palindromic sequences ('P nucleotides'); (ii) the introduction of additional nucleotides ('N additions') in the junction by the terminal deoxynucleotidyl transferase (TdT); (iii) exonucleolytic cleavage that results in the trimming of nucleotides at the boundary between the two coding ends (6).

Vγ9Vδ2 T cells express a TCR containing the γ-chain variable region 9 (Vγ9, TRGV9) and the δ-chain variable region 2 (Vδ2, TRDV2) and are the dominant population of γδ T cells in the blood circulation of human adults. They are activated and expanded in a TCR-dependent manner by microbe- and host-derived phosphorylated prenyl metabolites (phosphorylated antigens or 'phosphoantigens'), derived from the isoprenoid metabolic pathway (7, 8). Prototypical examples of phosphoantigens include the microbial (E)-4-hydroxy-3-methyl-but-2-enyl pyrophosphate (HMBPP) produced by the 2-C-methyl-D-erythritol 4-phosphate (MEP) or 'non-mevalonate' pathway of isoprenoid synthesis, and host isopentenyl pyrophosphate (IPP) generated via the mevalonate pathway. These phosphoantigens do not bind directly the Vγ9Vδ2 TCR but have been recently shown to be sensed by the butyrophilin BTN3A1 and, via a mechanism that is yet to be fully understood, activate indirectly the Vγ9Vδ2 T cells (8, 9). The recognition of phosphoantigens allows Vγ9Vδ2 T cells to develop potent antimicrobial immune responses or to promote the killing of transformed host cells that up-regulate IPP production, which has led to the development of clinical trials targeting Vγ9Vδ2 T cells as a cancer immunotherapy approach (4, 10–12).

In the mouse model, it is long established that innate γδ T cells develop in waves during fetal development (13, 14). These early innate γδ T cells express (semi-)invariant γδ TCRs, whereas later on in development the TCRs possess polyclonal CDR3 sequences(14). Representing the prime example of such an invariant TCR, the first γδ T cells to emerge in the murine fetal thymus express a fixed TCR composed of invariant TRGV5-TRGJ1 and invariant TRDV1-TRDD2-TRDJ2 CDR3 chains (Vγ5Vδ1 in short; nomenclature according to Heilig and Tonegawa(15)) and migrate to the skin epidermis where they become dendritic epidermal T cells (DETCs). Here they are maintained until adulthood by clonal self-

renewal (13, 14, 16–18). Among human γδ T cells, Vγ9Vδ2 T cells appear to be the prototypic innate γδ T cell subset since, in contrast to other subsets (such as Vδ1+ and Vγ9-Vδ2+), they express a semi-invariant TCR(19–23). We have shown that the human mid-gestational fetal peripheral blood is highly enriched for Vγ9Vδ2 T cells expressing such a semi-invariant TCR (20). Combined with the relative absence of the Vδ2 chain in the postnatal thymus (24–26) and the described similarities between the cord and adult blood Vγ9Vδ2 TCR repertoire (23), this suggests a fetal wave of Vγ9Vδ2 T cells that, as is the case for mouse innate γδ T cells, persist in adulthood by clonal expansion. However, other scenarios involving a post-natal thymic output as a source of the adult blood Vγ9Vδ2 T cells cannot be ruled out (27).

To track the lineage relationship of fetal and adult phosphoantigen-reactive Vγ9Vδ2 T cells, we analyzed in detail the CDR3 repertoire by high-throughput sequencing (HTS) of *ex vivo* sorted blood and thymus Vγ9+Vδ2+ γδ T cells from postnatal (birth until adult) and fetal subjects. This was complemented with the CDR3 repertoire analysis of HMBPP-expanded Vγ9Vδ2 thymocytes and of Vγ9Vδ2 T cells generated by hematopoietic-stem-and-precursor-cells (HSPC) *in vitro*. We found that adult blood Vγ9Vδ2 T cells are derived from the small number of Vγ9Vδ2 T cells generated in the postnatal thymus and, surprisingly, not from the abundant fetal population.

122 **Materials and Methods**

123

124 **Human cell material**

125 Human peripheral blood, thymus and liver samples were collected from the following sources where
126 all participants (when apply mothers/parents) gave written informed consent in accordance with the
127 Declaration of Helsinki. Fetal blood because of interruption of pregnancy (22-30 weeks of gestation),
128 approved by the Hôpital Erasme ethics committee; umbilical cord blood after delivery (vaginal) (39-41
129 weeks term delivery) with the approval of the University Hospital Center Saint-Pierre; adult peripheral
130 blood (>18years, 26-64 years), approved by the Ethics committee of the CHU Tivoli, La Louvière; fetal
131 thymus and fetal liver (15-21 weeks of estimated gestational age), approved by the Centralised
132 Institutional Research Board of the Singapore Health Services in Singapore; post-natal thymus obtained
133 from children (4 months to 8 years old) who underwent cardiac surgery and mobilized peripheral blood
134 samples of adult donors (for the OP9DL1 co-culture), approved by Medical Ethical Committee of Ghent
135 University Hospital.
136 Blood was layered over lymphoprep (Axis-Shield) with resulting PBMC cryopreserved for subsequent
137 experiments. Cell suspensions from fetal thymus and liver and post-natal thymus samples were
138 obtained as previously described(28, 29).

139

140 **Flow cytometry, sorting and cell cultures**

141 For flow cytometry and associated cell sorting, cells were thawed in complete medium, washed twice
142 and labelled with Zombie NIR™ dye (Biolegend), and the cells were then subsequently stained for cell
143 surface antigens with antibodies directed against CD3 (clone UCHT1, BD), TCR-γδ (11F2, BD), TCR-Vγ9
144 (IMMU360; Beckman Coulter), TCR-Vδ2 (IMMU389; Beckman Coulter). CD3+γδTCR+Vγ9+Vδ2+ were
145 sorted for "Vγ9Vδ2" (mean purity 98.0% of CD3+γδ+) and the rest CD3+ γδTCR+ non(Vγ9Vδ2) were
146 sorted for "nonVγ9Vδ2" γδ T cells (mean purity 98.6 % of CD3+γδ+) on a FACS Aria III (BD). Gating
147 strategy: FS singlets → alive cells (zombie negative) → SSC-FSC lymphocyte/thymocyte gate →
148 CD3+γδTCR+ → Vγ9 – Vδ2, Vγ9+Vδ2+ or non(Vγ9Vδ2). Data were analyzed using FlowJo software (Tree
149 Star).
150 For Vγ9Vδ2 T cell expansion experiments, post-natal thymocytes enriched for untouched γδ T cells
151 with the TCRγ/δ+ T Cell Isolation Kit (130-092-892, Miltenyi Biotec) were cultured for 10 days at 37 °C,
152 5% CO_2 in 14-mL polypropylene, round-bottom tubes (Falcon; BD) at a final concentration of 1 $\times 10^6$
153 cells/mL, in presence of HMBPP 10nM (Echelon Bioscience) and IL-2 100U/ml ((Proleukin,
154 Chiron/Novartis) which was added every 3 days. Culture medium consisted of RPMI 1640 (Gibco,

155 Invitrogen), supplemented with L-glutamine (2 mM), penicillin (50 U/mL), streptomycin (50 U/mL), and
156 1% nonessential amino acids (Lonza) and 10% (vol/vol) heat-inactivated FCS (PPA Laboratories).
157 Irradiated PBMC (30 min at 2400cGy) were used as feeders at the ratio of 1/1 in the cultures of
158 thymocytes. After expansion, Vγ9Vδ2 T cells were sorted as described above.
159 OP9DL1 cells were obtained from Dr. J. C. Zúñiga-Pflücker (University of Toronto, Canada)(30). Isolated
160 CD34+ cells were seeded in a 6-well culture plate (5x105 cells/well) containing a monolayer of OP9DL1
161 cells in MEMα (Minimum Essential Medium α) (Gibco, Life Technologies) supplemented with 20% fetal
162 bovine serum (Sigma), 1% NEAA, 1% Glutamine, 1% Pen/Strep (Lonza) in the presence of 10 ng/ml IL-
163 7 (R&D Systems), 10 ng/ml Flt3L (PeproTech) and 5 ng/ml SCF (PeproTech). Every 4-5 days cells were
164 harvested by vigorous pipetting and transferred in a new 6-well plate (between $5x10^5$-$1x10^6$
165 cells/well)(29). After ca. 30 days in co-culture with OP9-DL1 cells, HPSC-derived cells were snap frozen
166 in liquid nitrogen and stored at -80 C for later RNA extraction.
167

168 **TCRγ and TCRδ NGS**

169 RNA was isolated from sorted cells (usually 5000-15000 Vγ9Vδ2 T cells) with the RNeasy Micro Kit
170 (Qiagen) or from OP9DL1 co-cultures with the RNeasy Mini Kit (Qiagen). cDNA was generated
171 performing a template switch anchored RT-PCR. RNA was reverse transcribed via a template-switch
172 cDNA reaction using TRCG (5'- CAAGAAGACAAAGGTATGTTCCAG) and TRDC (5'-
173 GTAGAATTCCTTCACCAGACAAG) specific primers in the same reaction tube, a template-switch adaptor
174 (5'-AAGCAGTGGTATCAACGCAGAGTACATrGrGrG) and the Superscript II RT enzyme (Invitrogen). The
175 TRCG primer binds both TRCG1 and TRCG2. The cDNA was then purified using AMPure XP Beads
176 (Agencourt). Amplification of the TRG and TRD region was achieved using a specific TRGC primer
177 (binding also both TRCG1 and TRCG2 5'-
178 *GTCTCGTGGGCTCGGAGATGTGTATAAGAGACAG*AATAGTGGGCTTGGGGGAAACATCTGCAT, adapter in
179 italic) and a specific TRDC primer (5'-
180 *GTCTCGTGGGCTCGGAGATGTGTATAAGAGACAG*ACGGATGGTTTGGTATGAGGCTGACTTCT, adapter in
181 italic) and a primer complementary to the template-switch adapter (5'-
182 *TCGTCGGCAGCGTCAGATGTGTATAAGAGACAG*AAGCAGTGGTATCAACGCAG, adapter in italic) with the
183 KAPA Real-Time Library Amplification Kit (Kapa Biosystems). Adapters were required for subsequent
184 sequencing reactions. After purification with AMPure XP beads, an index PCR with Illumina sequencing
185 adapters was performed using the Nextera XT Index Kit. This second PCR product was again purified
186 with AMPure XP beads. High-throughput sequencing of the generated amplicon products containing
187 the TRG and TRD sequences was performed on an Illumina MiSeq platform using the V2 300 kit, with

188 150 base pairs (bp) at the 3' end (read 2) and 150 bp at the 5' end (read 1) [at the GIGA center,
189 University of Liège, Belgium].
190 Raw sequencing reads from fastq files (read 1 and read 2) were aligned to reference V, D and J genes
191 from GenBank database specifically for 'TRG' or 'TRD' to build CDR3 sequences using the MiXCR
192 software version 2.1.12.(31). Default parameters were used except to assemble TRDD gene segment
193 where 3 instead of 5 consecutive nucleotides were applied as assemble parameter. CDR3 sequences
194 were then exported and analyzed using VDJtools software version 1.2.1 using default settings(32).
195 Sequences out of frame and containing stop codons were excluded from the analysis. The CDR3
196 repertoire data shown are filtered for TRGV9 and TRDV2 sequences. Note that the nucleotype lengths
197 generated by VDJtools include the C and V ends of the CDR3 clonotypes. For OP9DL1 cultures, the
198 CDR3 repertoire was examined on total culture cells (and not on sorted Vγ9Vδ2 T cells), but we focused
199 on the TRGV9-TRGJP repertoire, as this TRGV-TRGJ combination is associated with phosphoantigen-
200 reactivity(33, 34). Tree maps were created using the Treemap Package (https://CRAN.R-
201 project.org/package=treemap). Conservation of TRGV9 and TRGJP sequences among primates was
202 investigated by using the genome browser at https://genome-euro.ucsc.edu/ (human assembly Dec.
203 2013 GRCh38/hg38) and its comparative genomics tool; the figure illustrating the conservation of
204 sequences was generated with the GeneRunner software.

205

206 **Statistical analysis**

207 All statistical analyses were performed using GraphPad Prism 6. Parametric tests were used after
208 verifying the normality of the data using the Kolmogorov-Smirnov normality test. Differences between
209 groups were analyzed using Kruskal–Wallis ANOVA and Dunn's post-tests for non-parametric data.
210 *P<0.05, **P<0.01, ***P<0.001.

211

212 **Results**

213

214 **Adult and fetal blood Vγ9Vδ2 T cells show a different CDR3 repertoire**

215 To verify whether adult blood Vγ9Vδ2 T cells can be derived from their counterparts in the fetal blood
216 circulation, we compared in detail the CDR3 repertoire of sorted adult, cord and fetal blood Vγ9Vδ2 T
217 cells by HTS. We used fetal blood derived from gestation ages 22-30 weeks when the Vγ9Vδ2 T cells
218 are highly enriched, cord blood from term delivery (39-41 weeks), by which time the Vδ1+ T cells
219 become the major γδ T cell population (20) and adult blood from healthy volunteers (18-65 years old).
220 First, we quantified the level of N additions in the CDR3 repertoire. Adult blood Vγ9Vδ2 T cells used
221 clearly many more N additions than fetal blood Vγ9Vδ2 T cells, both in their CDR3γ and CDR3δ
222 repertoire; cord blood Vγ9Vδ2 T cells used an intermediate number of N additions (Fig. 1a,
223 supplemental Fig. 1a). The mean CDR3 lengths were longer in adult compared to fetal Vγ9Vδ2 T cells
224 (Fig. 1b). The distribution of the CDR3γ was highly restricted towards the length corresponding to 14
225 aa +/-1 (or 48 nt +/-3, including C and F ends), matching phosphoantigen-reactive CDR3γ lengths(34),
226 both in fetal and adult blood Vγ9Vδ2 T cells (supplemental Fig. 1b, top panel). Since the differences in
227 CDR3 length were not as high as the differences in N additions would suggest (compare Fig. 1b with
228 Fig. 1a), we wondered whether differential J segment usage could contribute to the minimization of
229 the CDR3 length differences. For CDR3δ, we could indeed identify an enriched usage of TRDJ3 and
230 TRDJ2 in fetal blood Vγ9Vδ2 T cells which are 8 and 3 nucleotides longer than the adult prevalent TRDJ1
231 (Fig. 1c, bottom panel). The differences in N additions were maintained when only sequences using
232 'adult-type' TRDJ1 or 'fetal-type' TRDJ3 were analyzed (supplementary Fig. 1c). There was also a slight
233 increase in the usage of shorter TRDD1 (8 nucleotides) and TRDD2 (9 nucleotides) in adult compared
234 to fetal Vγ9Vδ2 T cells at the expense of the longer (13 nucleotides) TRDD3 (supplementary Fig. 2a). In
235 the CDR3γ repertoire however, the vast majority of the TRGV9 sequences in both fetal and adult blood
236 Vδ2+ (Fig. 1c top panel) but not of Vδ2- (supplementary Fig. 2b) γδ T cells used TRGJP, consistent with
237 the importance of this J gene segment for phosphoantigen-reactivity(33, 34). It seems that an increase
238 of nucleotide deletion (trimming) in the adult at the end of the TRGV9 gene segment (supplemental
239 Fig. 2c) is more likely to contribute to the conservation of the CDR3γ length (Fig. 1b, supplemental Fig.
240 1b).

241

242 The TRGV9 CDR3 repertoire was more focused than the TRDV2 CDR3 repertoire for all groups (Fig. 1
243 d,e). While there was some variability, the diversity of the fetal/cord and adult CDR3 TRDV2 repertoire
244 was broadly similar (Fig. 1d-e) as described previously (23). However, there was a significantly higher
245 CDR3 overlap within pairs of fetal compared to pairs of postnatal subjects (Fig. 1f). The higher sharing
246 within the fetal TRGV9 repertoire was in great part due to the high prevalence of the germline-encoded

247 nucleotype 5'-TGTGCCTTGTGGGAGGTGCAAGAGTTGGGCAAAAAAATCAAGGTATTT-3' (Fig. 1g),
248 encoding the clonotype CALWEVQELGKKIKVF at amino acid level, giving rise to a phosphoantigen-
249 reactive receptor(20). Furthermore, the CALWEVQELGKKIKF clonotype in the adult blood Vγ9Vδ2 T
250 cells was also encoded by alternative nucleotypes that included N additions, which could not be
251 detected in fetal blood Vγ9Vδ2 T cells (Fig. 1f, green bar). While CDR3δ sequence and length can be
252 variable in Vγ9Vδ2 T cells, it has been shown that the presence of a hydrophobic amino acid at position
253 5 of the CDR3δ is important for phosphoantigen reactivity, both in cord and adult blood-derived
254 Vγ9Vδ2 T cells(33–35). The percentage of Vγ9Vδ2 T cells expressing a hydrophobic residue (VILWFMC,
255 mainly V and L) at this position 5 was high in both fetal and adult blood Vγ9Vδ2 T cells (Fig. 1h),
256 independent of their TRDJ usage (supplemental Fig. 2d). However, analysis of the CDR3δ at the
257 nucleotype level revealed that in fetal blood Vγ9Vδ2 T cells the vast majority of nucleotypes use a
258 germline codon to encode this hydrophobic residue (Fig. 1h, black bars), while in more than half of
259 adult blood Vγ9Vδ2 T cells that particular codon contains N insertions (Fig. 1h, green bars).
260 In summary, both the CDR3γ and CDR3δ repertoire of fetal and blood Vγ9Vδ2 T cells show major
261 differences, including in how the features important for phosphoantigen reactivity are encoded.
262
263 **Expansion of phosphoantigen-reactive fetal blood Vγ9Vδ2 T cells does not lead to an adult-type**
264 **CDR3 repertoire**
265 To verify a possible selection upon microbial phosphoantigen exposure after birth, we expanded *in*
266 *vitro* fetal blood Vγ9Vδ2 T cells with the microbial-derived phosphoantigen HMBPP(20) and studied
267 the changes in the CDR3 repertoire. Despite a strong Vγ9Vδ2 T cell expansion(20), 'fetal-type' TRDJ3
268 was still the major TRDJ gene segment and no preferential expansion of the 'adult-type' TRDJ1 usage
269 could be observed (Fig. 2a). Note that a shift towards a TRDJ1 usage could already be seen before birth
270 (compare fetal (<30w gestation) and cord (>37w gestation) in Fig. 1c, bottom panel) which is in line
271 with a shift of TRDJ usage that is independent of microbial exposure after birth. Furthermore, the
272 percentage of the 'fetal' nucleotype 5'-
273 TGTGCCTTGTGGGAGGTGCAAGAGTTGGGCAAAAAAATCAAGGTATTT-3' (encoding the clonotype
274 CALWEVQELGKKIKVF) remained stable upon *in vitro* expansion with HMBPP (Fig. 2b) and there was no
275 shift towards a more adult-type CDR3 repertoire at the level of N insertions or sharing (Fig. 2c, 2d).
276 Based on these data, we conclude that it is unlikely that the adult blood Vγ9Vδ2 T cells are derived
277 from fetal blood Vγ9Vδ2 T cells expanded upon microbial exposure after birth.
278
279
280
281 **Fetal and post-natal Vγ9Vδ2 thymocytes express a different CDR3 repertoire**

282 In an effort to determine the origin of the adult blood Vγ9Vδ2 T cells, we carefully investigated the
283 presence of Vγ9+Vδ2+ cells within post-natal pediatric thymuses. It has been described previously that
284 Vδ2+ thymocytes are either absent or only present at a very low frequency, which contributed to the
285 notion that (adult) blood Vγ9Vδ2 T cells are derived from the fetal thymus (14, 24–26, 36–38). Indeed,
286 we found that the frequency of γδ thymocytes expressing the Vδ2 chain in the post-natal thymus is
287 significantly lower compared to the fetal thymus, but they are clearly present (supplementary Fig. 3a,
288 Fig. 3a, bottom panel). Importantly, a large fraction of the post-natal Vδ2+ thymocytes co-expressed
289 the Vγ9 chain (supplementary Fig. 3a) resulting in about 6% of the post-natal γδ thymocytes being
290 Vγ9+Vδ2+ (Fig. 3a). Taking into account the more than 20-fold increase in size of the organ between
291 fetal week 20 and the age of 5 and the 5-fold reduction in percentage, it can be assumed that both the
292 fetal and post-natal thymus produce and export Vγ9+Vδ2+ T cells. Thus, we sorted fetal and post-natal
293 Vγ9+Vδ2+ thymocytes and compared their CDR3 repertoire.
294 Like in the fetal versus adult blood Vγ9Vδ2 comparison, the post-natal thymic Vγ9Vδ2 repertoire,
295 compared to the fetal counterpart, contained significantly more N additions (Fig. 3b, supplementary
296 Fig. 3b), had longer CDR3δ (Fig. 3b bottom panel, supplementary Fig. 3c), showed more trimming at
297 the TRGV9 end (supplementary Fig. 3d top panel) and preferentially used TRDJ1 and TRDD1/TRDD2
298 (Fig.3d bottom panel; supplementary Fig. 3e). Like in the blood Vγ9Vδ2 repertoire, the CDR3γ length
299 distribution was more focused than the CDR3δ repertoire, both in the fetal and post-natal Vγ9Vδ2
300 thymocytes (supplementary Fig. 3c). Of note, TRGJP was the main TRGJ gene segment used both by
301 fetal and post-natal thymic Vγ9Vδ2 T cells (Fig. 3d top panel) but the percentage was lower than in
302 their peripheral blood counterparts (compare Fig. 3d with Fig. 1c), as observed previously in thymic
303 versus blood Vγ9Vδ2 T cell clones (35). In contrast, the TRGV9 chain of Vγ9+Vδ2- thymocytes was
304 mainly combined with the TRGJ1/2 gene segment (supplementary Fig. 3f, top panel), like in the
305 periphery (supplementary Fig. 2b, left panel). The higher diversity of the post-natal Vγ9Vδ2 thymocytes
306 (Fig. 3e, f) contributed to a much lower repertoire overlap within post-natal subjects compared to the
307 overlap within fetal subjects (Fig. 3g). The high sharing within the fetal thymic TRGV9 repertoire was
308 in great part due to the high prevalence of the public canonical germline-encoded nucleotype (Fig. 3g
309 right top panel). In the post-natal Vγ9Vδ2 thymocytes, this public nucleotype was also present but it
310 was less abundant in subjects older than 4 months (Fig 3h). Moreover, the hydrophobic amino acid at
311 position 5 was more encoded by N-containing codons in the post-natal compared to the fetal Vγ9Vδ2
312 thymocytes (Fig. 3i). Of note, both the fetal and post-natal Vγ9Vδ2 thymocytes contained a lower
313 percentage of TRDV2-containing CDR3δ possessing a hydrophobic amino acid at position 5 (Fig. 3i)
314 compared to their blood counterparts (Fig. 1h).

315 In summary, the post-natal thymic Vγ9Vδ2 TCR repertoire differs from its fetal counterpart in all
316 parameters that differed in blood derived Vγ9Vδ2 T cells and resembles the adult blood Vγ9Vδ2
317 repertoire.
318
319 **Recombination of the germline-encoded public TRGV9-TRJP CDR3 sequence**
320 The high abundance of the public germline-encoded invariant CDR3γ sequence 5'-5'-
321 TGTGCCTTGTGGGAGGTGCAAGAGTTGGGCAAAAAAATCAAGGTATTT-3' -3' in both the fetal blood and
322 fetal thymus Vγ9Vδ2 T cells triggered us to investigate the mechanism of its rearrangement. The lack
323 of N additions in the fetal repertoire may provide a favorable setting for the usage of short-homology
324 repeats to generate invariant CDR3 as described for mouse innate γδ T cells (39, 40). Furthermore, P
325 nucleotides can be involved in such a mechanism of invariant CDR3 generation (39). We found that the
326 addition of two P nucleotides at the end of the TRGV9 region generates a GCA sequence which is also
327 found in the TRGJP region, and only in this TRGJ region (Fig 4a-b). This model explains the preferential
328 recombination of the 5'-TGTGCCTTGTGGGAGGTGCAAGAGTTGGGCAAAAAAATCAAGGTATTT-3' to
329 encode CALWEVQELGKKIKVF in the absence of N additions in the fetus. In later life, when N additions
330 are involved, the public TRGV9-TRGJP amino acid sequence CALWEVQELGKKIKVF can still be produced
331 by other nucleotypes (Fig. 4c)(27) but its prevalence is much lower, as previously discussed (Fig. 1g).
332 Strikingly, the nucleotides involved in this short-homology recombination are highly conserved among
333 a series of non-human primate species (Fig. 4d), except for the TRGJP gene of orangutan, which is a
334 pseudogene(41).
335
336 **HMBPP-expanded post-natal Vγ9Vδ2 thymocytes express an adult blood-type CDR3 repertoire**
337 The post-natal thymic Vγ9Vδ2 TCR repertoire (Fig. 3) resembled the adult blood Vγ9Vδ2 repertoire
338 (Fig. 1), suggesting that the adult blood Vγ9Vδ2 T cells are post-natal thymus-derived and expand in
339 the periphery upon microbial phosphoantigen exposure after birth. In order to test this hypothesis, we
340 expanded post-natal Vγ9Vδ2 thymocytes with the microbial-derived phosphoantigen HMBPP and
341 analyzed their CDR3 repertoire comparing it to the adult blood repertoire. We observed high specific
342 expansion of the Vγ9Vδ2 thymocytes upon stimulation with HMBPP (Fig. 5a), as previously observed
343 with exposure towards heat-killed *Mycobacterium tuberculosis* (42). The level of mean N additions did
344 not change upon expansion (Fig 5b). In contrast, there was an increase in the TRGJP usage till adult
345 blood-type levels accounting at the same time for an increase of the TRGV9 CDR3 length compared to
346 *ex vivo* thymocytes (Fig 5c, d). Notably, the CDR3γ and CDR3δ diversity of the expanded Vγ9Vδ2
347 thymocytes became very similar to the adult blood repertoire (Fig 5e, f) consistent with the focusing
348 of the repertoire in the periphery.

349 No major differences were observed upon HMBPP-induced expansion regarding the overlap frequency
350 of the repertoire and the abundance of the public TRGV9 clonotype (*CALWEVQELGKKIKVF*) which was
351 already similar between *ex vivo* Vγ9Vδ2 thymocytes and adult blood Vγ9Vδ2 T cells (Fig. 5g, h). In sharp
352 contrast, HMBPP-mediated expansion increased the percentage of the TRDV2 repertoire using at
353 position 5 a hydrophobic residue, a feature important for phosphoantigen-reactivity (33–35),
354 approaching adult blood-type levels (Fig. 5i).
355 In summary, post-natal Vγ9Vδ2 thymocytes are able to expand upon phosphoantigen exposure and
356 acquire a CDR3 repertoire that closely resembles that of adult blood Vγ9Vδ2 T cells unlike the
357 expanded fetal blood Vγ9Vδ2 T cells.
358
359 **The generation of fetal-like or adult-like Vγ9Vδ2 T cells is HSPC-dependent**
360 To investigate whether the differences between the fetal versus post-natal Vγ9Vδ2 thymocyte
361 repertoire were caused by different properties of the fetal and postnatal hematopoietic precursor cells
362 or rather by extrinsic factors such as intrathymic exposure to phosphoantigens, we cultured
363 hematopoietic precursor cells from a spectrum of sources (fetal liver, fetal blood, cord blood, and adult
364 blood) in the OP9DL1 *in vitro* T cell development system to generate γδ T cells(29). Although at a low
365 level, Vγ9+Vδ2+ γδ T cells could be generated using this system and their prevalence was inversely
366 proportional to the age of the HSPC source (Fig. 6a). Strikingly, the mean number of N additions within
367 the TRGV9-TRGJP repertoire increased from almost zero, when using fetal liver as the HSPC source, to
368 2-4 N insertions, when cord or adult blood HPSC were used (Fig. 6b). These numbers are very similar
369 to what is observed in *ex vivo* sorted Vγ9Vδ2 thymocytes (Fig. 3b; supplementary Fig. 3b). Furthermore,
370 the public canonical TRGV9-TRGJP nucleotype was generated very efficiently by fetal-derived HSPC
371 (fetal liver and fetal blood) but only poorly by adult-derived HSPC; cord blood-derived HSPC generated
372 intermediate percentages (Fig. 6c). Likewise, in the adult/cord HSPC-derived CDR3δ repertoire, there
373 were more TRDV2-containing CDR3δ sequences that used N-additions to encode the hydrophobic
374 amino acid at position 5 (Fig 6d). Taken together, these data indicate that the HSPC source, fetal or
375 later life, drives the generation of the Vγ9Vδ2 T cells towards a fetal- or adult-type repertoire.
376
377

378 **Discussion**

379

380 In the last few years, fate-mapping in mouse models has revealed the developmental origins of various
381 immune cell types, including the DETC innate γδ T cell subset (18, 43, 44). However, such fate-mapping
382 approach is not possible for the innate phosphoantigen-reactive Vγ9Vδ2 T cells since these cells do not
383 exist in rodents (45). In this study, we used CDR3 HTS to track human Vγ9Vδ2 T cells and discovered
384 that, unlike adult mouse innate γδ T cells which are generated in a single fetal wave, the development
385 of Vγ9Vδ2 T cells continues after birth resulting in the adult Vγ9Vδ2 TCR repertoire.

386

387 Our data contrast with the hypothesis that the adult blood Vγ9Vδ2 repertoire is derived by selection
388 after birth from the fetal-generated Vγ9Vδ2 T cells (20, 23). As we studied fetal and postnatal thymus,
389 we could show that the adult-type blood Vγ9Vδ2 TCR repertoire (e.g. a private repertoire with a higher
390 number of N insertions) was present in the post-natal but not in the fetal thymus. In addition,
391 phosphoantigen selection *in vitro* by microbial-derived HMBPP further sculptured the postnatal thymic
392 repertoire to a very similar repertoire as found in the adult blood (e.g. further enrichment of TRGJP
393 usage). Therefore we believe that the adult blood Vγ9Vδ2 repertoire is generated in the postnatal
394 rather than the fetal thymus and is further selected in the periphery by microbial phosphoantigen
395 exposure. The HMBPP-induced selection of the adult Vγ9Vδ2 TCR repertoire is consistent with the
396 higher response of adult Vγ9Vδ2 T cells compared to their fetal counterparts upon stimulation *in vitro*
397 with HMBPP (20, 46). The distinct development in the fetal versus post-natal thymus could be
398 mimicked in the *in vitro* T cell development system OP9DL1: the fetal canonical CDR3γ nucleotype
399 (TRGV9-TRGJP 5'-TGTGCCTTGTGGGAGGTGCAAGAGTTGGGCAAAAAAATCAAGGTATTT-3' , encoding the
400 clonotype CALWEVQELGKKIKF) was generated much more efficiently by fetal-derived HSPC compared
401 to post-natal-derived HSPC, thus indicating that stem/precursor cell autonomous properties underpin
402 this distinct development. While we found that the canonical CDR3γ nucleotype and associated
403 clonotype is highly prevalent in early life and less in the adult, it appears that the situation for the
404 canonical CDR3α (defined by selected usage of TRAV, TRAJ and restricted CDR3 length) of human
405 mucosal-associated invariant T (MAIT) cells, another main innate T cell subset, is the opposite: the
406 canonical MAIT TCR is more frequent in adult than in cord blood MAIT cells (47). This difference
407 between cord and adult MAIT cells appears to be due to antigen-driven expansion (47), rather than by
408 a distinct development as found here for fetal/cord versus adult Vγ9Vδ2 T cells.

409

410 In both fetal and adult blood Vγ9Vδ2 T cells the TRGV9-TRGJP pairing and CDR3γ length restriction was
411 conserved, consistent with the demonstration that these features are essential for phosphoantigen-
412 reactivity(33, 34). This is also compatible with the notion that the Vγ9Vδ2 TCR can be regarded as a

413 pattern recognition receptor and that Vγ9Vδ2 T cells are the main innate γδ T cell subset in human (21,
414 23, 48). However, our data highlighted a series of differences in the CDR3γ repertoire of fetal and adult
415 Vγ9Vδ2 T cells. While the germline-encoded and phosphoantigen-reactive canonical TRGV9-TRGJP
416 nucleotype was present both in early and later life, it was much more prevalent in the fetal blood
417 Vγ9Vδ2 repertoire. This nucleotype has been described to occupy more than 45% of all CDR3γ
418 sequences in the adult blood circulation, but a more recent study (21) reported a much lower
419 percentage (4% of all CDR3γ) consistent with our findings in the adult blood. We propose that the
420 absence of N insertions in the fetal Vγ9Vδ2 thymocyte repertoire allows the usage of a short-homology
421 repeat (GCA, germline-encoded in the TRGJP and generated via the addition of P nucleotides in TRGV9)
422 driving the recombination of the TRGV9-TRGJP nucleotype 5'-
423 TGTGCCTTGTGGGAGGTGCAAGAGTTGGGCAAAAAAATCAAGGTATTT-3' , resulting in its high prevalence
424 in the fetus. In the adult, N additions prevent this short-homology repeat-mediated recombination(40)
425 and rather generate public N-containing phosphoantigen-reactive CDR3γ sequences via convergent
426 recombination(27), consistent with a different origin of the fetal and adult Vγ9Vδ2 T cells. We found
427 that the TRGV9-TRGJP GCA short-homology repeat is highly conserved among primates, similar to the
428 conservation of amino acid residues important for phosphoantigen reactivity(41, 49, 50). Based on the
429 high evolutionary conservation of the short-homology-generated germline-encoded TRGV9-TRGJP
430 nucleotype and its high prevalence in the fetus, we propose that protection against congenital
431 infections with HMBPP-producing pathogens such as *Plasmodium falciparum*, *Toxoplasma gondii*,
432 *Treponema pallidum* or *Brucella abortus*(7, 51–53)), has provided a selective pressure for a germline-
433 encoded phosphoantigen-reactive TCR early during fetal development(54) and that the short-
434 homology repeat identified here contributes to the efficient generation of such a TCR.
435
436 The TRDV2-associated CDR3 length was much more variable compared to the CDR3γ. Despite this
437 variation, the amino acid at position 5 was highly enriched for a hydrophobic residue, both in fetal and
438 adult blood Vγ9Vδ2 T cells, consistent with its importance for phosphoantigen-reactivity (33, 34). But
439 the coding of this particular hydrophobic acid was germ-line based in the fetus, while in the adult a
440 large fraction was formed by N-containing codons, thus again consistent with a distinct development
441 of fetal and adult Vγ9Vδ2 T cells. In addition, the CDR3δ of fetal blood Vγ9Vδ2 T cells were strikingly
442 enriched for TRDJ3 usage while adult blood Vγ9Vδ2 T cells mainly used TRDJ1. A recent HTS study
443 based on sorted Vδ2+ T cells (thus containing both Vγ9+Vδ2+ and Vγ9-Vδ2+ cells) found that the
444 enriched cord blood TRDV2-TRDJ3 CDR3 sequences contained only a low percentage of a hydrophobic
445 residue at position 5 (23). It has been suggested that this contributes to the low phosphoantigen-
446 reactivity of cord blood Vγ9Vδ2 T cells and thus to the high enrichment of TRDJ1 in adult Vγ9Vδ2 T
447 cells after birth upon phosphoantigen exposure (23). However, we found that both the TRDV2-TRDJ1

448 and TRDV3-TRDJ3 CDR3 sequences of sorted Vγ9Vδ2 T cells were enriched for a hydrophobic amino
449 acid at this position. Furthermore, *in vitro* expansion with the microbe-derived phosphoantigen
450 HMBPP did not result in a bias towards TRDJ1 usage, which is consistent with the enrichment of the
451 hydrophobic amino acid in both TRDJ3- and TRDJ1-containing CDR3δ sequences.
452
453 Our data highlight the importance of several Vγ9Vδ2 TCR features for phosphoantigen-reactivity as
454 they are conserved in fetal and adult life regardless of the distinct way these features are encoded.
455 Despite the major advancement of the discovery of BTN3A1 as a crucial protein in the activation of
456 Vγ9Vδ2 T cells with phosphoantigens, the exact mechanism of interaction with the Vγ9Vδ2 TCR is yet
457 to be revealed (8). Thus it is also unclear what the exact role of the TRGJP sequence is, in particular the
458 conserved amino acids important for phosphoantigen reactivity (33, 34, 45, 50), why a restricted
459 CDR3γ length of 14 +/- 1 aa is needed and what the role is of the hydrophobic amino acid at position 5
460 of the CDR3δ. Indeed, it remains to be established what the direct ligand is of the Vγ9Vδ2 TCR and thus
461 the potential interacting domains with these CDR3γ and CDR3δ features (8).
462
463 Our data may have implications for immunotherapeutic approaches that target Vγ9Vδ2 T cells.
464 Although the *in vivo* expansion of Vγ9Vδ2 T cells by phosphoantigens or nitrogen-containing
465 bisphosphonates such as zoledronate has been translated to early-phase clinical trials, problems such
466 as activation-induced Vγ9Vδ2 T cell anergy and a decrease in the number of peripheral blood Vγ9Vδ2
467 T cells after infusion of these stimulants have not yet been solved (10–12). In addition, it is difficult to
468 expand *ex vivo* Vγ9Vδ2 T cells from advanced cancer patients with decreased initial numbers of
469 peripheral blood Vγ9Vδ2 T cells (11). This is important as favorable clinical outcomes are related to
470 higher frequency of peripheral blood Vγ9Vδ2 T cells (10, 11). Thus novel approaches are needed to
471 stably expand and maintain the responsiveness and functions of Vγ9Vδ2 T cells. Since our data strongly
472 indicate that Vγ9Vδ2 T cells within the blood circulation of adults are derived post-natally, strategies
473 could be developed to enhance *de novo* generation of Vγ9Vδ2 T cells in cancer patients (55, 56).
474

Acknowledgments

We are grateful to the mothers that participated in this study and the midwives of the Hospital Erasme (ULB) and CHU Saint-Pierre delivery room that helped to the recruitment of the mothers. We thank the GIGA Genomics platform (Latifa Karim and Wouter Coppieters) for their outstanding technical support and Damien Debot for his help with the CDR3 analysis.

Author contributions

MP and PT designed and undertook experiments; NM, JKYC, FGo, GG, ND, AC, CD, FGi and BV designed, prepared and provided critical human cell material; MP and DV processed and interpreted data; MP, BV and DV wrote the manuscript and DV designed the study.

Competing interests

The authors declare no competing interests.

489 **References**
490

491 1. Hayday, A. C. 2000. [gamma][delta] cells: a right time and a right place for a conserved third way of
492 protection. *Annu.Rev.Immunol.* 18: 975–1026.
493 2. Chien, Y., C. Meyer, and M. Bonneville. 2014. γδ T cells: first line of defense and beyond. *Annu.*
494 *Rev. Immunol.* 32: 121–155.
495 3. Vantourout, P., and A. Hayday. 2013. Six-of-the-best: unique contributions of gammadelta T cells
496 to immunology. *Nat.Rev.Immunol.* 13: 88–100.
497 4. Silva-Santos, B., K. Serre, and H. Norell. 2015. γδ T cells in cancer. *Nat. Rev. Immunol.* 15: 683–691.
498 5. Chien, Y. H., and Y. Konigshofer. 2007. Antigen recognition by gammadelta T cells. *Immunol.Rev.*
499 215: 46–58.
500 6. Notarangelo, L. D., M.-S. Kim, J. E. Walter, and Y. N. Lee. 2016. Human RAG mutations:
501 biochemistry and clinical implications. *Nat. Rev. Immunol.* 16: 234–246.
502 7. Eberl, M., M. Hintz, A. Reichenberg, A. K. Kollas, J. Wiesner, and H. Jomaa. 2003. Microbial
503 isoprenoid biosynthesis and human gammadelta T cell activation. *FEBS Lett* 544: 4–10.
504 8. Boutin, L., and E. Scotet. 2018. Towards Deciphering the Hidden Mechanisms That Contribute to
505 the Antigenic Activation Process of Human Vγ9Vδ2 T Cells. *Front. Immunol.* 9.
506 9. Vermijlen, D., D. Gatti, A. Kouzeli, T. Rus, and M. Eberl. 2018. γδ T cell responses: How many
507 ligands will it take till we know? *Semin. Cell Dev. Biol.* 84: 75–86.
508 10. Fournié, J.-J., H. Sicard, M. Poupot, C. Bezombes, A. Blanc, F. Romagné, L. Ysebaert, and G.
509 Laurent. 2013. What lessons can be learned from γδ T cell-based cancer immunotherapy trials? *Cell.*
510 *Mol. Immunol.* 10: 35–41.
511 11. Kobayashi, H., and Y. Tanaka. 2015. gammadelta T Cell Immunotherapy-A Review.
512 *Pharmaceuticals.(Basel)* 8: 40–61.
513 12. Lo Presti, E., G. Pizzolato, E. Gulotta, G. Cocorullo, G. Gulotta, F. Dieli, and S. Meraviglia. 2017.
514 Current Advances in γδ T Cell-Based Tumor Immunotherapy. *Front. Immunol.* 8: 1401.
515 13. Carding, S. R., and P. J. Egan. 2002. Gammadelta T cells: functional plasticity and heterogeneity.
516 *Nat.Rev.Immunol.* 2: 336–345.
517 14. Vermijlen, D., and I. Prinz. 2014. Ontogeny of Innate T Lymphocytes - Some Innate Lymphocytes
518 are More Innate than Others. *Front Immunol* 5: 486.
519 15. Heilig, J. S., and S. Tonegawa. 1986. Diversity of murine gamma genes and expression in fetal and
520 adult T lymphocytes. *Nature* 322: 836–840.
521 16. Havran, W. L., and J. P. Allison. 1988. Developmentally ordered appearance of thymocytes
522 expressing different T-cell antigen receptors. *Nature* 335: 443–445.
523 17. Ikuta, K., T. Kina, I. MacNeil, N. Uchida, B. Peault, Y. H. Chien, and I. L. Weissman. 1990. A
524 developmental switch in thymic lymphocyte maturation potential occurs at the level of
525 hematopoietic stem cells. *Cell* 62: 863–874.
526 18. Gentek, R., C. Ghigo, G. Hoeffel, A. Jorquera, R. Msallam, S. Wienert, F. Klauschen, F. Ginhoux,
527 and M. Bajénoff. 2018. Epidermal γδ T cells originate from yolk sac hematopoiesis and clonally self-
528 renew in the adult. *J. Exp. Med.* 215: 2994–3005.
529 19. Sherwood, A. M., C. Desmarais, R. J. Livingston, J. Andriesen, M. Haussler, C. S. Carlson, and H.
530 Robins. 2011. Deep sequencing of the human TCRgamma and TCRbeta repertoires suggests that
531 TCRbeta rearranges after alphabeta and gammadelta T cell commitment. *Sci.Transl.Med.* 3: 90ra61.
532 20. Dimova, T., M. Brouwer, F. Gosselin, J. Tassignon, O. Leo, C. Donner, A. Marchant, and D.
533 Vermijlen. 2015. Effector Vgamma9Vdelta2 T cells dominate the human fetal gammadelta T-cell
534 repertoire. *Proc.Natl.Acad.Sci.U.S.A* .
535 21. Ravens, S., C. Schultze-Florey, S. Raha, I. Sandrock, M. Drenker, L. Oberdörfer, A. Reinhardt, I.
536 Ravens, M. Beck, R. Geffers, C. von Kaisenberg, M. Heuser, F. Thol, A. Ganser, R. Förster, C.
537 Koenecke, and I. Prinz. 2017. Human γδ T cells are quickly reconstituted after stem-cell
538 transplantation and show adaptive clonal expansion in response to viral infection. *Nat. Immunol.*
539 18: 393–401.

22. Davey, M. S., C. R. Willcox, S. P. Joyce, K. Ladell, S. A. Kasatskaya, J. E. McLaren, S. Hunter, M. Salim, F. Mohammed, D. A. Price, D. M. Chudakov, and B. E. Willcox. 2017. Clonal selection in the human Vδ1 T cell repertoire indicates γδ TCR-dependent adaptive immune surveillance. *Nat. Commun.* 8: 14760.
23. Davey, M. S., C. R. Willcox, S. Hunter, S. A. Kasatskaya, E. B. M. Remmerswaal, M. Salim, F. Mohammed, F. J. Bemelman, D. M. Chudakov, Y. H. Oo, and B. E. Willcox. 2018. The human Vδ2+ T-cell compartment comprises distinct innate-like Vγ9+ and adaptive Vγ9- subsets. *Nat. Commun.* 9: 1760.
24. Parker, C. M., V. Groh, H. Band, S. A. Porcelli, C. Morita, M. Fabbi, D. Glass, J. L. Strominger, and M. B. Brenner. 1990. Evidence for extrathymic changes in the T cell receptor gamma/delta repertoire. *J.Exp.Med.* 171: 1597–1612.
25. McVay, L. D., S. R. Carding, K. Bottomly, and A. C. Hayday. 1991. Regulated expression and structure of T cell receptor gamma/delta transcripts in human thymic ontogeny. *EMBO J* 10: 83–91.
26. Ribot, J. C., S. T. Ribeiro, D. V. Correia, A. E. Sousa, and B. Silva-Santos. 2014. Human gammadelta thymocytes are functionally immature and differentiate into cytotoxic type 1 effector T cells upon IL-2/IL-15 signaling. *J.Immunol.* 192: 2237–2243.
27. Willcox, C. R., M. S. Davey, and B. E. Willcox. 2018. Development and Selection of the Human Vγ9Vδ2+ T-Cell Repertoire. *Front. Immunol.* 9.
28. McGovern, N., A. Shin, G. Low, D. Low, K. Duan, L. J. Yao, R. Msallam, I. Low, N. B. Shadan, H. R. Sumatoh, E. Soon, J. Lum, E. Mok, S. Hubert, P. See, E. H. Kunxiang, Y. H. Lee, B. Janela, M. Choolani, C. N. Z. Mattar, Y. Fan, T. K. H. Lim, D. K. H. Chan, K.-K. Tan, J. K. C. Tam, C. Schuster, A. Elbe-Bürger, X.-N. Wang, V. Bigley, M. Collin, M. Haniffa, A. Schlitzer, M. Poidinger, S. Albani, A. Larbi, E. W. Newell, J. K. Y. Chan, and F. Ginhoux. 2017. Human fetal dendritic cells promote prenatal T-cell immune suppression through arginase-2. *Nature* 546: 662–666.
29. Van Coppernolle, S., G. Verstichel, F. Timmermans, I. Velghe, D. Vermijlen, M. De Smedt, G. Leclercq, J. Plum, T. Taghon, B. Vandekerckhove, and T. Kerre. 2009. Functionally mature CD4 and CD8 TCRalphabeta cells are generated in OP9-DL1 cultures from human CD34+ hematopoietic cells. *J.Immunol.* 183: 4859–4870.
30. La Motte-Mohs, R. N., E. Herer, and J. C. Zúñiga-Pflücker. 2005. Induction of T-cell development from human cord blood hematopoietic stem cells by Delta-like 1 in vitro. *Blood* 105: 1431–1439.
31. Bolotin, D. A., S. Poslavsky, I. Mitrophanov, M. Shugay, I. Z. Mamedov, E. V. Putintseva, and D. M. Chudakov. 2015. MiXCR: software for comprehensive adaptive immunity profiling. *Nat. Methods* 12: 380–381.
32. Shugay, M., D. V. Bagaev, M. A. Turchaninova, D. A. Bolotin, O. V. Britanova, E. V. Putintseva, M. V. Pogorelyy, V. I. Nazarov, I. V. Zvyagin, V. I. Kirgizova, K. I. Kirgizov, E. V. Skorobogatova, and D. M. Chudakov. 2015. VDJtools: Unifying Post-analysis of T Cell Receptor Repertoires. *PLoS Comput. Biol.* 11: e1004503.
33. Yamashita, S. 2003. Recognition mechanism of non-peptide antigens by human T cells. *Int. Immunol.* 15: 1301–1307.
34. Wang, H., Z. Fang, and C. T. Morita. 2010. Vgamma2Vdelta2 T Cell Receptor recognition of prenyl pyrophosphates is dependent on all CDRs. *J.Immunol.* 184: 6209–6222.
35. Davodeau, F., M. A. Peyrat, M. M. Hallet, I. Houde, H. Vie, and M. Bonneville. 1993. Peripheral selection of antigen receptor junctional features in a major human gamma delta subset. *Eur.J.Immunol.* 23: 804–808.
36. Casorati, G., G. De Libero, A. Lanzavecchia, and N. Migone. 1989. Molecular analysis of human gamma/delta+ clones from thymus and peripheral blood. *J. Exp. Med.* 170: 1521–1535.
37. Krangel, M. S., H. Yssel, C. Brocklehurst, and H. Spits. 1990. A distinct wave of human T cell receptor gamma/delta lymphocytes in the early fetal thymus: evidence for controlled gene rearrangement and cytokine production. *J.Exp.Med.* 172: 847–859.
38. McVay, L. D., S. S. Jaswal, C. Kennedy, A. Hayday, and S. R. Carding. 1998. The generation of human gammadelta T cell repertoires during fetal development. *J.Immunol.* 160: 5851–5860.

591 39. Itohara, S., P. Mombaerts, J. Lafaille, J. Iacomini, A. Nelson, A. R. Clarke, M. L. Hooper, A. Farr, and
592 S. Tonegawa. 1993. T cell receptor delta gene mutant mice: independent generation of alpha beta T
593 cells and programmed rearrangements of gamma delta TCR genes. *Cell* 72: 337–348.
594 40. Zhang, Y., D. Cado, D. M. Asarnow, T. Komori, F. W. Alt, D. H. Raulet, and J. P. Allison. 1995. The
595 role of short homology repeats and TdT in generation of the invariant gamma delta antigen
596 receptor repertoire in the fetal thymus. *Immunity* 3: 439–447.
597 41. Kazen, A. R., and E. J. Adams. 2011. Evolution of the V, D, and J gene segments used in the
598 primate gammadelta T-cell receptor reveals a dichotomy of conservation and diversity. *Proc. Natl.*
599 *Acad. Sci. U. S. A.* 108: E332-340.
600 42. Kabelitz, D., A. Bender, T. Prospero, S. Wesselborg, O. Janssen, and K. Pechhold. 1991. The
601 primary response of human gamma/delta + T cells to Mycobacterium tuberculosis is restricted to V
602 gamma 9-bearing cells. *J. Exp. Med.* 173: 1331–1338.
603 43. Smith, N. L., R. K. Patel, A. Reynaldi, J. K. Grenier, J. Wang, N. B. Watson, K. Nzingha, K. J. Yee
604 Mon, S. A. Peng, A. Grimson, M. P. Davenport, and B. D. Rudd. 2018. Developmental Origin Governs
605 CD8+ T Cell Fate Decisions during Infection. *Cell* 174: 117–130.e14.
606 44. Gentek, R., C. Ghigo, G. Hoeffel, M. J. Bulle, R. Msallam, G. Gautier, P. Launay, J. Chen, F. Ginhoux,
607 and M. Bajénoff. 2018. Hemogenic Endothelial Fate Mapping Reveals Dual Developmental Origin of
608 Mast Cells. *Immunity* 48: 1160–1171.e5.
609 45. Karunakaran, M. M., T. W. Gobel, L. Starick, L. Walter, and T. Herrmann. 2014. Vgamma9 and
610 Vdelta2 T cell antigen receptor genes and butyrophilin 3 (BTN3) emerged with placental mammals
611 and are concomitantly preserved in selected species like alpaca (Vicugna pacos). *Immunogenetics*
612 66: 243–254.
613 46. Moens, E., M. Brouwer, T. Dimova, M. Goldman, F. Willems, and D. Vermijlen. 2011. IL-23R and
614 TCR signaling drives the generation of neonatal Vgamma9Vdelta2 T cells expressing high levels of
615 cytotoxic mediators and producing IFN-gamma and IL-17. *J.Leukoc.Biol.* 89: 743–752.
616 47. Ben Youssef, G., M. Tourret, M. Salou, L. Ghazarian, V. Houdouin, S. Mondot, Y. Mburu, M.
617 Lambert, S. Azarnoush, J.-S. Diana, A.-L. Virlouvet, M. Peuchmaur, T. Schmitz, J.-H. Dalle, O. Lantz, V.
618 Biran, and S. Caillat-Zucman. 2018. Ontogeny of human mucosal-associated invariant T cells and
619 related T cell subsets. *J. Exp. Med.* 215: 459–479.
620 48. Liuzzi, A. R., J. E. McLaren, D. A. Price, and M. Eberl. 2015. Early innate responses to pathogens:
621 pattern recognition by unconventional human T-cells. *Curr. Opin. Immunol.* 36: 31–37.
622 49. Wang, H., H. K. Lee, J. F. Bukowski, H. Li, R. A. Mariuzza, Z. W. Chen, K.-H. Nam, and C. T. Morita.
623 2003. Conservation of Nonpeptide Antigen Recognition by Rhesus Monkey V 2V 2 T Cells. *J.*
624 *Immunol.* 170: 3696–3706.
625 50. Pauza, C. D., and C. Cairo. 2015. Evolution and function of the TCR Vgamma9 chain repertoire: It's
626 good to be public. *Cell. Immunol.* 296: 22–30.
627 51. Klein, J. O., C. . Baker, J. S. Remington, and C. B. Wilson. 2006. Current concepts of infections of
628 the fetus and newborn infant. In *Infectious disease of the fetus and newborn infant* J. S. Remington,
629 and J. O. Klein, eds. Elsevier Saunders, Philadelphia, Pennsylvania, USA. 3–25.
630 52. Cairo, C., N. Longinaker, G. Cappelli, R. G. Leke, M. M. Ondo, R. Djokam, J. Fogako, R. J. Leke, B.
631 Sagnia, S. Sosso, V. Colizzi, and C. D. Pauza. 2014. Cord Blood Vgamma2Vdelta2 T Cells Provide a
632 Molecular Marker for the Influence of Pregnancy-Associated Malaria on Neonatal Immunity.
633 *J.Infect.Dis.* 209: 1653–1662.
634 53. Prugnolle, F., P. Durand, C. Neel, B. Ollomo, F. J. Ayala, C. Arnathau, L. Etienne, E. Mpoudi-Ngole,
635 D. Nkoghe, E. Leroy, E. Delaporte, M. Peeters, and F. Renaud. 2010. African great apes are natural
636 hosts of multiple related malaria species, including Plasmodium falciparum. *Proc. Natl. Acad. Sci.*
637 107: 1458–1463.
638 54. McVay, L. D., and S. R. Carding. 1996. Extrathymic origin of human gamma delta T cells during
639 fetal development. *J.Immunol.* 157: 2873–2882.
640 55. Roh, K.-H., and K. Roy. 2016. Engineering approaches for regeneration of T lymphopoiesis.
641 *Biomater. Res.* 20: 20.

642 56. Wang, C., W. Sun, Y. Ye, H. N. Bomba, and Z. Gu. 2017. Bioengineering of Artificial Antigen
643 Presenting Cells and Lymphoid Organs. *Theranostics* 7: 3504–3516.
644

645 **Figure legends**

646

647 **Fig. 1** Adult and fetal blood Vγ9Vδ2 T cells show major differences in their CDR3γ and CDR3δ
648 repertoire. **a-c** Comparison of the CDR3 TRGV9 (top row) and TRDV2 (bottom row) repertoire of
649 sorted Vγ9Vδ2 T cells derived from fetal, cord and adult peripheral blood: **a** Number of N additions,
650 each dot represents the weighted mean of an individual sample, **b** CDR3 length in nucleotides
651 (including the codons for C-start and F-end residues), each dot represents the weighted mean of an
652 individual sample, **c** J gene segment usage distribution. **d** Treemaps show CDR3 clonotype usage in
653 relation to TRGV9 (left) and TRDV2 (right) repertoire size in sorted Vγ9Vδ2 T cells from one
654 representative fetal, cord and adult blood subject (rectangle colors are chosen randomly and do not
655 match between plots). **e-h** Comparison of the CDR3 TRGV9 (top row) and TRDV2 (bottom row)
656 repertoire of sorted Vγ9Vδ2 T cells from fetal, cord and adult peripheral blood: **e** Accumulated
657 frequency curves generated from the 10 most prevalent clonotypes, **f** Comparison of geometric
658 mean of relative overlap frequencies (F metrics by VDJ tools) within pairs of fetal, of cord and of
659 adult blood subjects, each dot represents the F value of a pair of samples; **g** Comparison of
660 prevalence of the TRGV9-TRGJP clonotype CALWEVQELGKKIKVF encoded without N additions in
661 black (5'-TGTGCCTTGTGGGAGGTGCAAGAGTTGGGCAAAAAAATCAAGGTATTT-3') or encoded with N
662 additions in green, and **h** Percentage of the TRDV2 repertoire containing at position 5 of the CDR3δ a
663 highly hydrophobic residue (V, I, L, W, F, M or C): residue encoded without N additions in black or by
664 N addition(s) in green. Data shown from independent subjects, sorted Vγ9Vδ2 T cells from fetal
665 (n=5), cord (n=6) and adult peripheral blood (n=8). Error bars indicate means ± SEM.

666 **Fig. 2** Expansion of phosphoantigen-reactive fetal blood Vγ9Vδ2 T cells does not lead to an adult-type
667 CDR3 repertoire. **a-d** Comparison of the CDR3 repertoire of Vγ9Vδ2 T cells from *ex-vivo* fetal blood
668 (n=5) or from expanded with HMBPP (10 days) fetal blood (FB expanded, n=4): **a** TRDJ usage
669 distribution in the TRDV2 repertoire, **b** Prevalence of the public TRGV9-TRGJP clonotype
670 CALWEVQELGKKIKVF encoded without N additions (5'-
671 TGTGCCTTGTGGGAGGTGCAAGAGTTGGGCAAAAAAATCAAGGTATTT-3') in the TRGV9 repertoire, **c**
672 Number of N additions, each dot represents the weighted mean of an individual sample and **d**
673 Overlap frequencies of pairs of *ex-vivo or* expanded fetal blood in the TRGV9 (top) and TRDV2
674 (bottom) repertoire. Data shown from independent subjects (*ex-vivo* fetal blood shown also in Fig.1).
675 Error bars indicate means ± SEM.

676 **Fig. 3** Fetal and post-natal Vγ9Vδ2 thymocytes express a different CDR3 repertoire. **a** Percentage of
677 Vγ9+Vδ2+ cells in γδ+ thymocytes in fetal (n=4) and post-natal thymus (PN Thymus, n=10) (top);
678 representative flow cytometry plot of post-natal γδ thymocytes (bottom). **b-d:** Comparison of the

679 CDR3 TRGV9 (top row) and TRDV2 (bottom row) repertoire of sorted Vγ9Vδ2 T cells in Fetal Thymus
680 (n=3) and PN Thymus (n=3): **b** Number of N additions, each dot represents the weighted mean of an
681 individual sample, **c** CDR3 length in nucleotides (including the C-start and F-end residues), each dot
682 represents the weighted mean of an individual sample, and **d** J gene segment usage distribution. **e**
683 Tree-maps of CDR3 TRGV9 (left) and TRDV2 (right) repertoire of fetal (top) and post-natal (bottom)
684 Vγ9+Vδ2+ thymocytes (rectangle colors are chosen randomly and do not match between plots). **f-i**
685 Comparison of the CDR3 TRGV9 (top row) and TRDV2 (bottom row) repertoire of sorted Vγ9Vδ2 T
686 cells in Fetal Thymus (n=3) and PN Thymus (n=3): **f** Accumulated frequency curves generated from
687 the 10 most prevalent clonotypes, **g** Geometric mean of relative overlap frequencies (F metrics of
688 VDJ tools) within pairs of fetal thymus and of post-natal thymus (left), each dot represents the F
689 value of a pair of samples, and shared clonotype abundance plots (right) for two fetal thymus
690 samples (top 20 clonotypes shared in distinct colors, collapsed in dark grey and non-overlapping in
691 light grey), **h** Percentage of the TRGV9-TRGJP clonotype CALWEVQELGKKIKVF encoded without N
692 additions (5'-TGTGCCTTGTGGGAGGTGCAAGAGTTGGGCAAAAAAATCAAGGTATTT-3') in the TRGV9
693 repertoire. **i** Percentage of the TRDV2 repertoire containing at position 5 of the CDR3δ chain a highly
694 hydrophobic residue (V, I, L, W, F, M or C): residue encoded without N additions in black or encoded
695 by N addition(s) in green. Data shown from independent subjects. Error bars indicate means ± SEM.

696 **Fig. 4** Recombination of the germline-encoded public TRGV9-TRGJP CDR3 sequence via the short-
697 homology repeat GCA. **a** Sequence of the 3' end of TRGV9 and all possible TRGJ 5' regions. **b** Short-
698 homology repeats (gca) direct the site of recombination when TRGV9 joins TRGJP, to form the highly
699 prevalent 5'-TGTGCCTTGTGGGAGGTGCAAGAGTTGGGCAAAAAAATCAAGGTATTT-3' clonotype in
700 absence of N additions (scissors: endonuclease activity; AA: amino acid). **c** Nucleotypes containing
701 nucleotide insertions (N underlined, P in italics) encoding the TRGV9-TRGJP clonotype
702 CALWEVQELGKKIKVF. **d** Conservation of the nucleotide sequence gca in primates: the great apes *Pan*
703 *troglodyte*s (chimp) and *Pongo pygmaeus* (orangutan, here TRGJP is a pseudogene), the new-world
704 monkeys *Macaca mulatta* (rhesus) and *Macaca fascicularis* (crab-eating macaque) and the old-world
705 monkeys *Aotus nancymaae* (ma's night monkey) and *Callithrix jacchus* (marmoset).

706 **Fig. 5** HMBPP-expanded post-natal Vγ9Vδ2 thymocytes express an adult blood-type CDR3 repertoire.
707 **a** Expansion of post-natal Vγ9Vδ2 thymocytes after exposure to HMBPP (10nM) in presence of IL-2
708 (100U/ml) for 10 days. Graph shows the percentage of Vγ9+Vδ2+ cells of total thymocytes in culture,
709 in medium control (+IL-2) and HMBPP (+IL-2) at day 10. Flow cytometry plots representative of 3
710 subjects. **b-d** CDR3 TRGV9 (top row) and TRDV2 (bottom row) repertoire analysis in expanded
711 Vγ9Vδ2 thymocytes compared to *ex-vivo* post-natal thymic and adult blood Vγ9Vδ2: **b** Number of N
712 additions, each dot represents the weighted mean of an individual sample, **c** CDR3 length (nucleotide

713 count including the C-start and F-end residues), each dot represents the weighted mean of an
714 individual sample, and **d** J usage distribution. **e** Treemaps show CDR3 clonotype usage in relation to
715 TRGV9 (left) and TRDV2 (right) repertoire size in sorted expanded post-natal Vγ9Vδ2 thymocytes (PT
716 expanded) (rectangle colors are chosen randomly and do not match between plots). **f-i** CDR3 TRGV9
717 (top row) and TRDV2 (bottom row) repertoire analysis in expanded Vγ9Vδ2 thymocytes compared to
718 *ex-vivo* post-natal thymic and adult blood Vγ9Vδ2: **f** Accumulated frequency curves generated from
719 the 10 most prevalent clonotypes, **g** Geometric mean of relative overlap frequencies (F metrics of
720 VDJ tools) within pairs of PN thymus, PT expanded and adult blood, each dot represents the F value
721 of a pair of samples, **h** Percentage of the public TRGV9-TRGJP clonotype CALWEVQELGKKIKVF
722 encoded without N additions in black (5'-
723 TGTGCCTTGTGGGAGGTGCAAGAGTTGGGCAAAAAAATCAAGGTATTT-3') or encoded with N additions
724 in green and **i,** Percentage of the TRDV2 repertoire containing at the position 5 of the CDR3δ a highly
725 hydrophobic residue (V, I, L, W, F, M, C): residue encoded without N additions in black or encoded by
726 N addition(s) in green. Data shown from independent subjects, sorted Vγ9Vδ2 from post-natal
727 thymus after HMBPP expansion "PT expanded" n=3 , ex-vivo post-natal thymus "PN Thymus" n=3
728 (results also shown in Fig.4), ex-vivo adult blood "Adult Blood" n=8 (results also shown in Fig.1). Error
729 bars indicate means ± SEM.

730 **Fig. 6** The generation of fetal- versus adult-like Vγ9Vδ2 T cells is HSPC- dependent.
731 **a**. Percentage of Vγ9+Vδ2+ of γδ T cells produced in OP9DL1 cultures by fetal liver (FL, n=3), fetal
732 blood (FB, n=8), cord blood (CB, n=10) and adult blood (MB, n=3) HSPC at day 30 of culture. **b-d**
733 Comparison of the CDR3 TRGV9 and TRDV2 repertoire from the OP9DL1 cultures: **b** Number of N
734 additions, each dot represents the weighted mean of an individual sample and, **c** Prevalence of the
735 public TRGV9-TRGJP clonotype CALWEVQELGKKIKVF encoded without N additions (5'-
736 TGTGCCTTGTGGGAGGTGCAAGAGTTGGGCAAAAAAATCAAGGTATTT-3') within the TRGV9-TRGJP
737 repertoire; **d** Percentage of repertoire where the residue at position 5 was N-encoded out of the
738 TRDV2 repertoire containing at position a highly hydrophobic residue (V, I, L, W, F, M or C). Error bars
739 indicate means ± SEM.

740

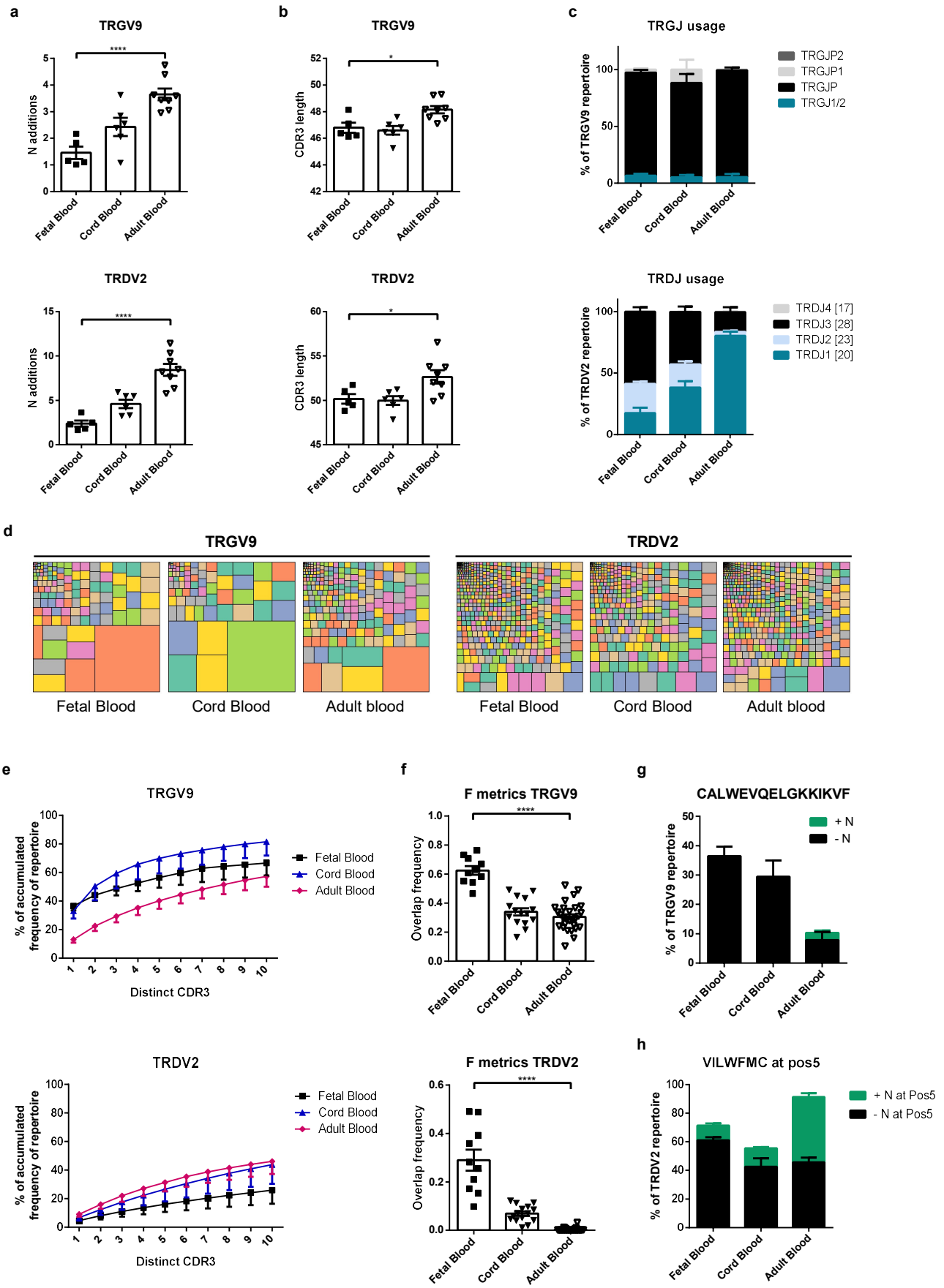
a
TRGV9
N additions
Fetal Blood
Cord Blood
Adult Blood
b
TRGV9
CDR3 length
c
TRGJ usage
% of TRGV9 repertoire
TRGJP2
TRGJP1
TRGJP
TRGJ1/2
TRDV2
TRDJ usage
% of TRDV2 repertoire
TRDJ4 [17]
TRDJ3 [28]
TRDJ2 [23]
TRDJ1 [20]
d
TRGV9
TRDV2
Fetal Blood
Cord Blood
Adult blood
e
TRGV9
% of accumulated frequency of repertoire
Distinct CDR3
Fetal Blood
Cord Blood
Adult Blood
TRDV2
f
F metrics TRGV9
Overlap frequency
F metrics TRDV2
g
CALWEVQELGKKIKVF
+ N
- N
% of TRGV9 repertoire
h
VILWFMC at pos5
+ N at Pos5
- N at Pos5
% of TRDV2 repertoire

Figure 1

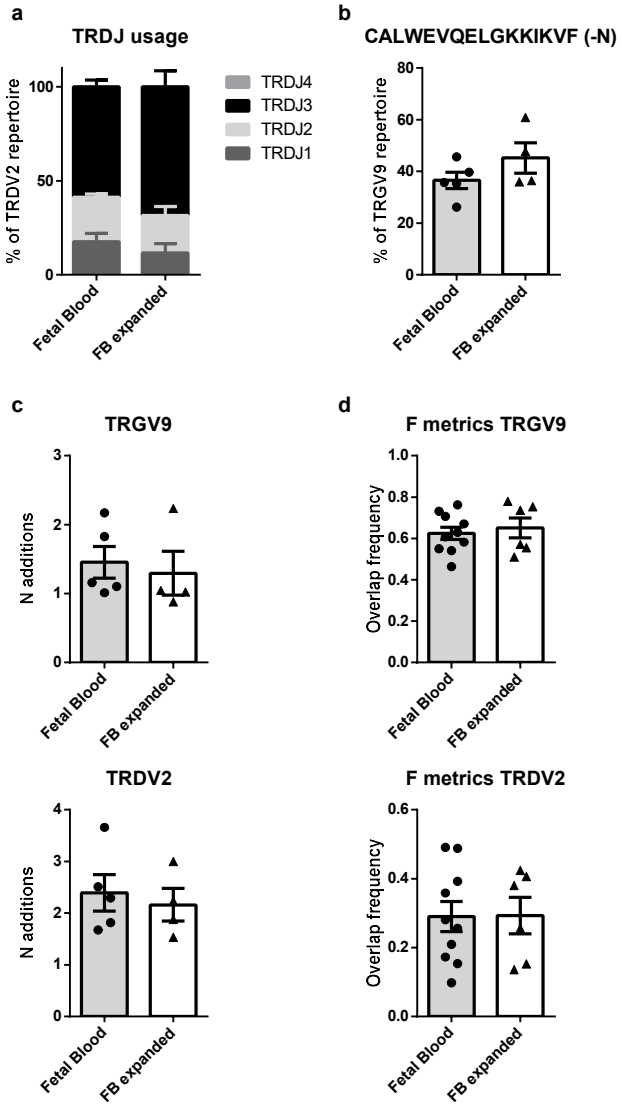
a
TRDJ usage
% of TRDV2 repertoire
100
50
0
TRDJ4
TRDJ3
TRDJ2
TRDJ1
Fetal Blood
FB expanded
b
CALWEVQELGKKIKVF (-N)
% of TRGV9 repertoire
80
60
40
20
0
Fetal Blood
FB expanded
c
TRGV9
N additions
3
2
1
0
Fetal Blood
FB expanded
d
F metrics TRGV9
Overlap frequency
1.0
0.8
0.6
0.4
0.2
0.0
Fetal Blood
FB expanded
TRDV2
N additions
4
3
2
1
0
Fetal Blood
FB expanded
F metrics TRDV2
Overlap frequency
0.6
0.4
0.2
0.0
Fetal Blood
FB expanded

Figure 2

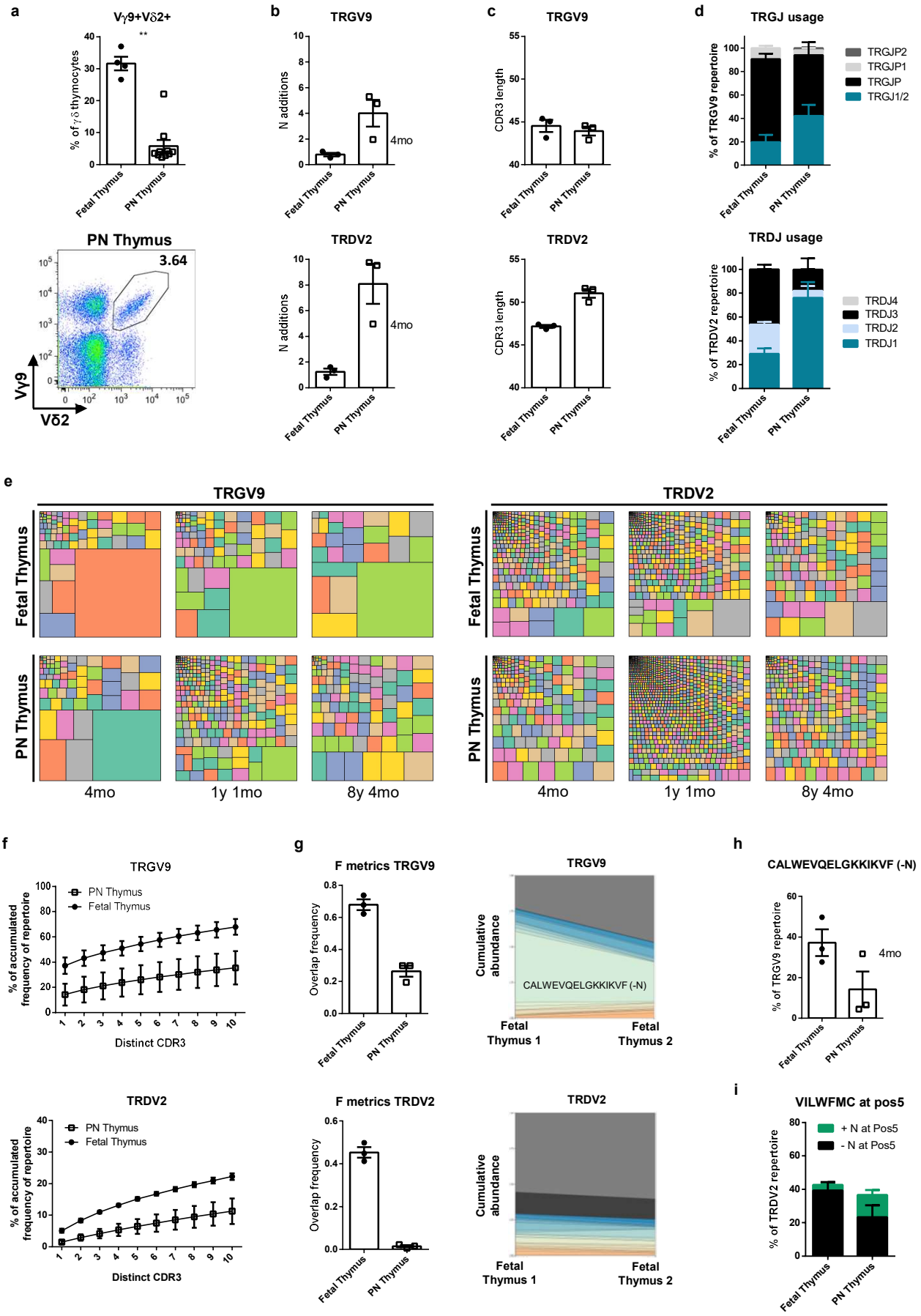
a
Vγ9+Vδ2+
% of γδ thymocytes
Fetal Thymus
PN Thymus
PN Thymus
3.64
Vγ9
Vδ2
b
TRGV9
N additions
4mo
TRDV2
c
TRGV9
CDR3 length
TRDV2
d
TRGJ usage
% of TRGV9 repertoire
TRGJP2
TRGJP1
TRGJP
TRGJ1/2
TRDJ usage
% of TRDV2 repertoire
TRDJ4
TRDJ3
TRDJ2
TRDJ1
e
TRGV9
TRDV2
Fetal Thymus
PN Thymus
4mo
1y 1mo
8y 4mo
f
TRGV9
PN Thymus
Fetal Thymus
% of accumulated frequency of repertoire
Distinct CDR3
TRDV2
g
F metrics TRGV9
Overlap frequency
TRGV9
Cumulative abundance
CALWEVQELGKKIKVF (-N)
Fetal Thymus 1
Fetal Thymus 2
F metrics TRDV2
TRDV2
h
CALWEVQELGKKIKVF (-N)
% of TRGV9 repertoire
i
VILWFMC at pos5
+ N at Pos5
- N at Pos5
% of TRDV2 repertoire

Figure 3

a

3' TRGV9 region

TGTGCCTTGTGGGAGGTG

5' TRGJ regions

TRGJ1 GAATTATTATAAGAAACTCTTT
TRGJ2 GAATTATTATAAGAAACTCTTT
TRGJP TGG**GCA**AGAGTTGGGCAAAAAAATCAAGGTATTT
TRGJP1 ATACCACTGGTTGGTTCAAGATATTT
TRGJP2 ATAGTAGTGATTGGATCAAGACGTTT

b

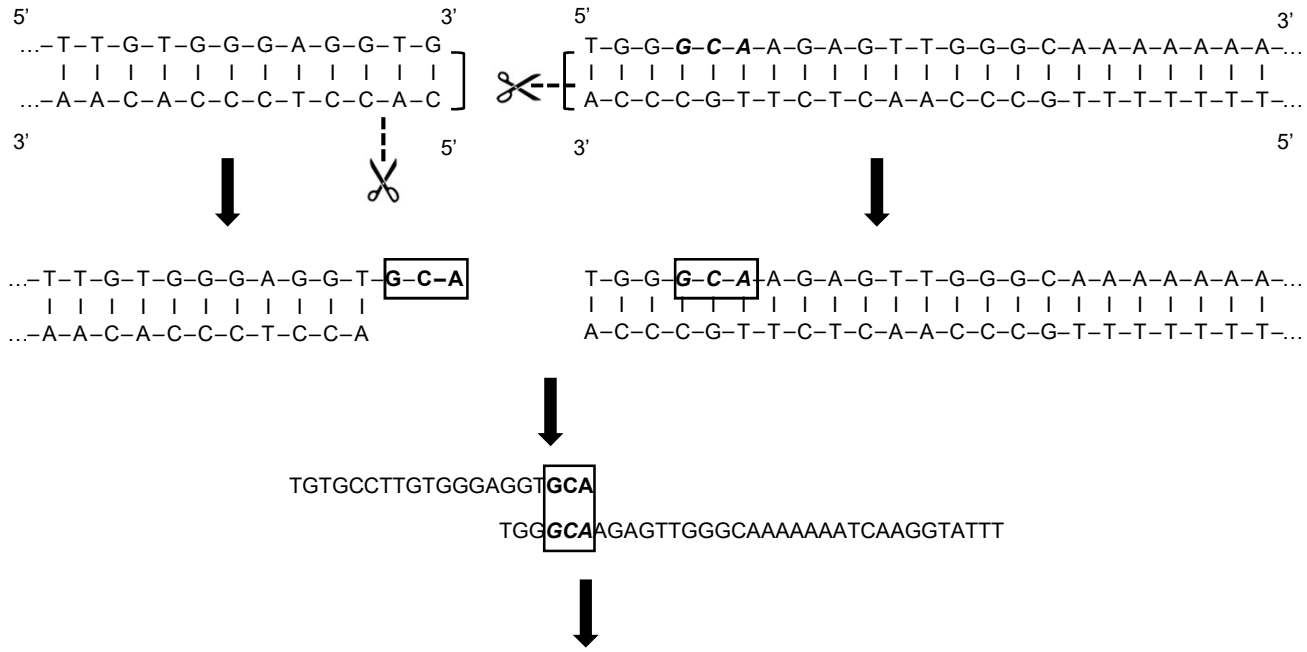

Nucleotype	TGT	GCC	TTG	TGG	GAG	GT**G**	**CA**A	GAG	TTG	GGC	AAA	AAA	ATC	AAG	GTA	TTT
AA sequence	C	A	L	W	E	V	Q	E	L	G	K	K	I	K	V	F

c

Amino-acid sequence	**C**	**A**	**L**	**W**	**E**	**V**	**Q**	**E**	**L**	**G**	**K**	**K**	**I**	**K**	**V**	**F**
Nucleotype 1	TGT	GCC	TTG	TGG	GAG	**GTT**	**CAA**	GAG	TTG	GGC	AAA	AAA	ATC	AAG	GTA	TTT
Nucleotype 2	TGT	GCC	TTG	TGG	GAG	**GTA**	**CAA**	GAG	TTG	GGC	AAA	AAA	ATC	AAG	GTA	TTT
Nucleotype 3	TGT	GCC	TTG	TGG	GAG	**GTC**	**CAA**	GAG	TTG	GGC	AAA	AAA	ATC	AAG	GTA	TTT
Nucleotype 4	TGT	GCC	TTG	TGG	GAG	**GTG**	***CAG***	GAG	TTG	GGC	AAA	AAA	ATC	AAG	GTA	TTT

d

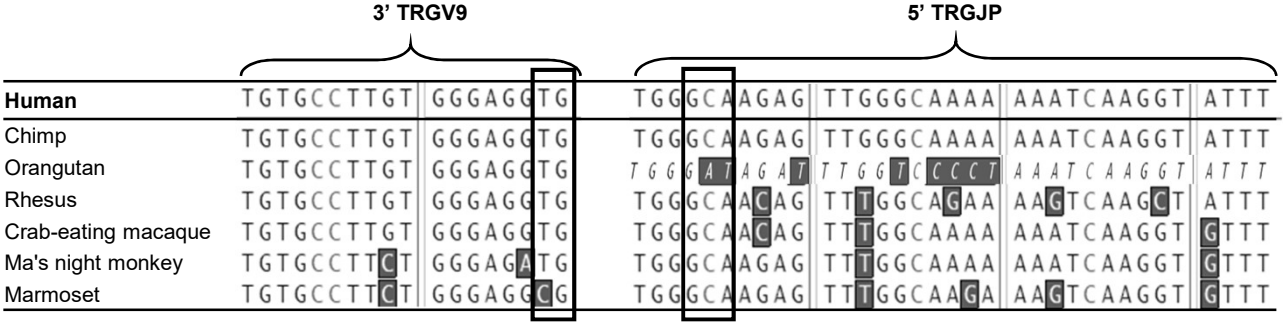

Figure 4

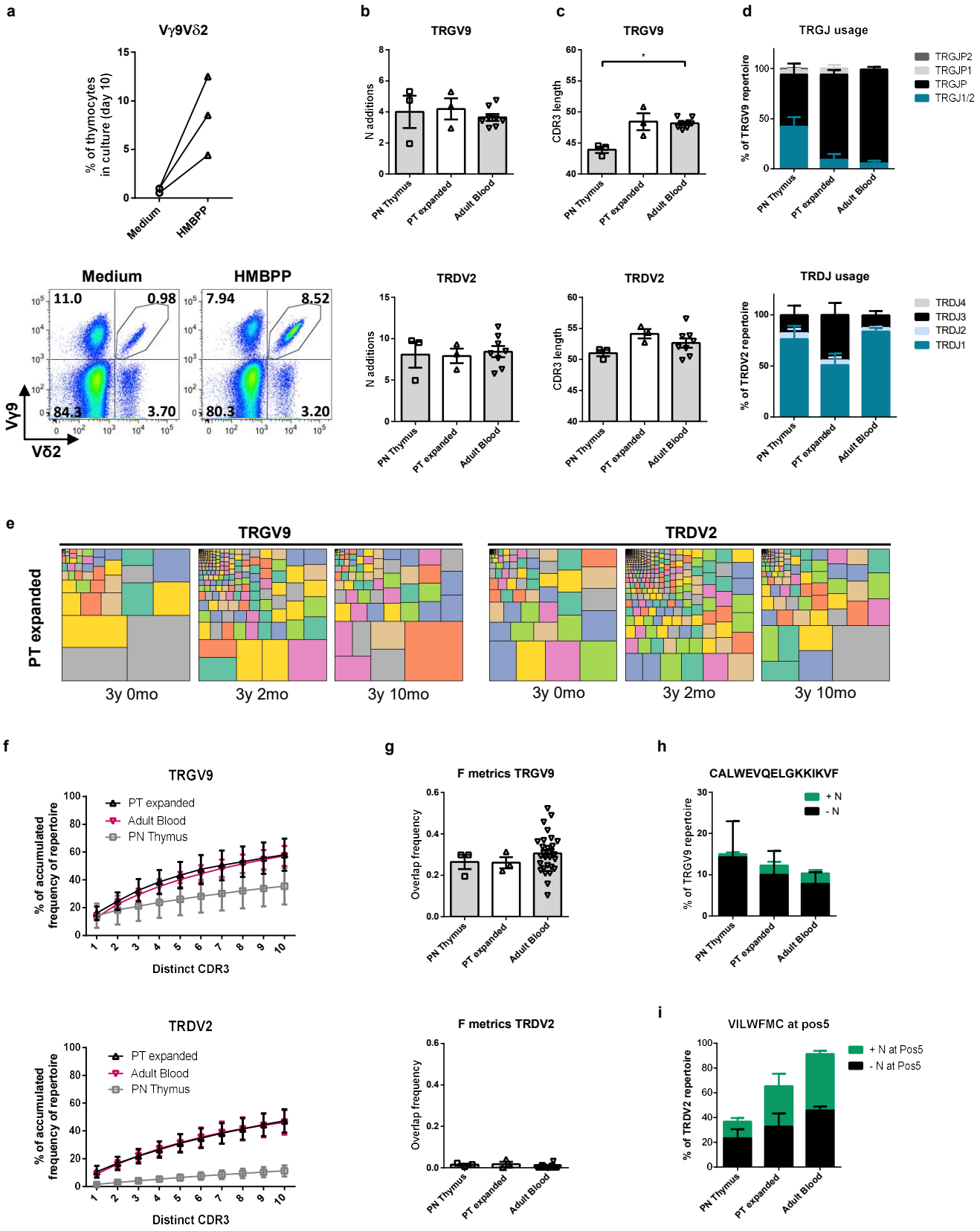
a
Vγ9Vδ2
% of thymocytes in culture (day 10)
Medium
HMBPP
Medium
HMBPP
11.0
0.98
84.3
3.70
7.94
8.52
80.3
3.20
Vγ9
Vδ2
b
TRGV9
N additions
PN Thymus
PT expanded
Adult Blood
TRDV2
N additions
c
TRGV9
CDR3 length
TRDV2
CDR3 length
d
TRGJ usage
% of TRGV9 repertoire
TRGJP2
TRGJP1
TRGJP
TRGJ1/2
TRDJ usage
% of TRDV2 repertoire
TRDJ4
TRDJ3
TRDJ2
TRDJ1
e
TRGV9
TRDV2
PT expanded
3y 0mo
3y 2mo
3y 10mo
f
TRGV9
% of accumulated frequency of repertoire
PT expanded
Adult Blood
PN Thymus
Distinct CDR3
TRDV2
g
F metrics TRGV9
Overlap frequency
F metrics TRDV2
h
CALWEVQELGKKIKVF
% of TRGV9 repertoire
+ N
- N
i
VILWFMC at pos5
% of TRDV2 repertoire
+ N at Pos5
- N at Pos5

Figure 5

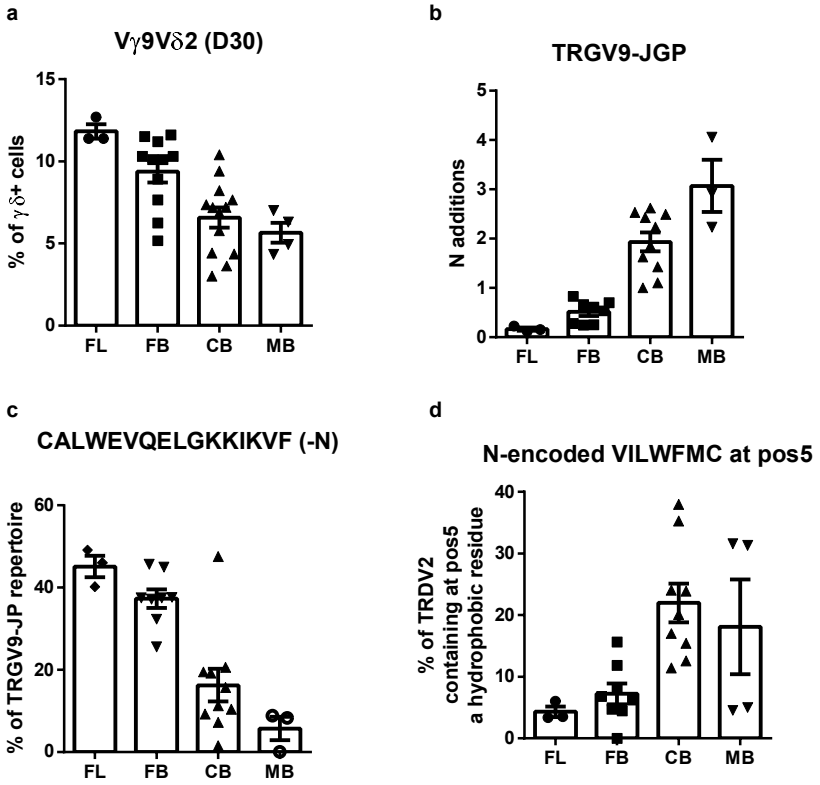
a
Vγ9Vδ2 (D30)
% of γδ+ cells
15
10
5
0
FL
FB
CB
MB
b
TRGV9-JGP
N additions
5
4
3
2
1
0
FL
FB
CB
MB
c
CALWEVQELGKKIKVF (-N)
% of TRGV9-JP repertoire
60
40
20
0
FL
FB
CB
MB
d
N-encoded VILWFMC at pos5
% of TRDV2 containing at pos5 a hydrophobic residue
40
30
20
10
0
FL
FB
CB
MB

Figure 6

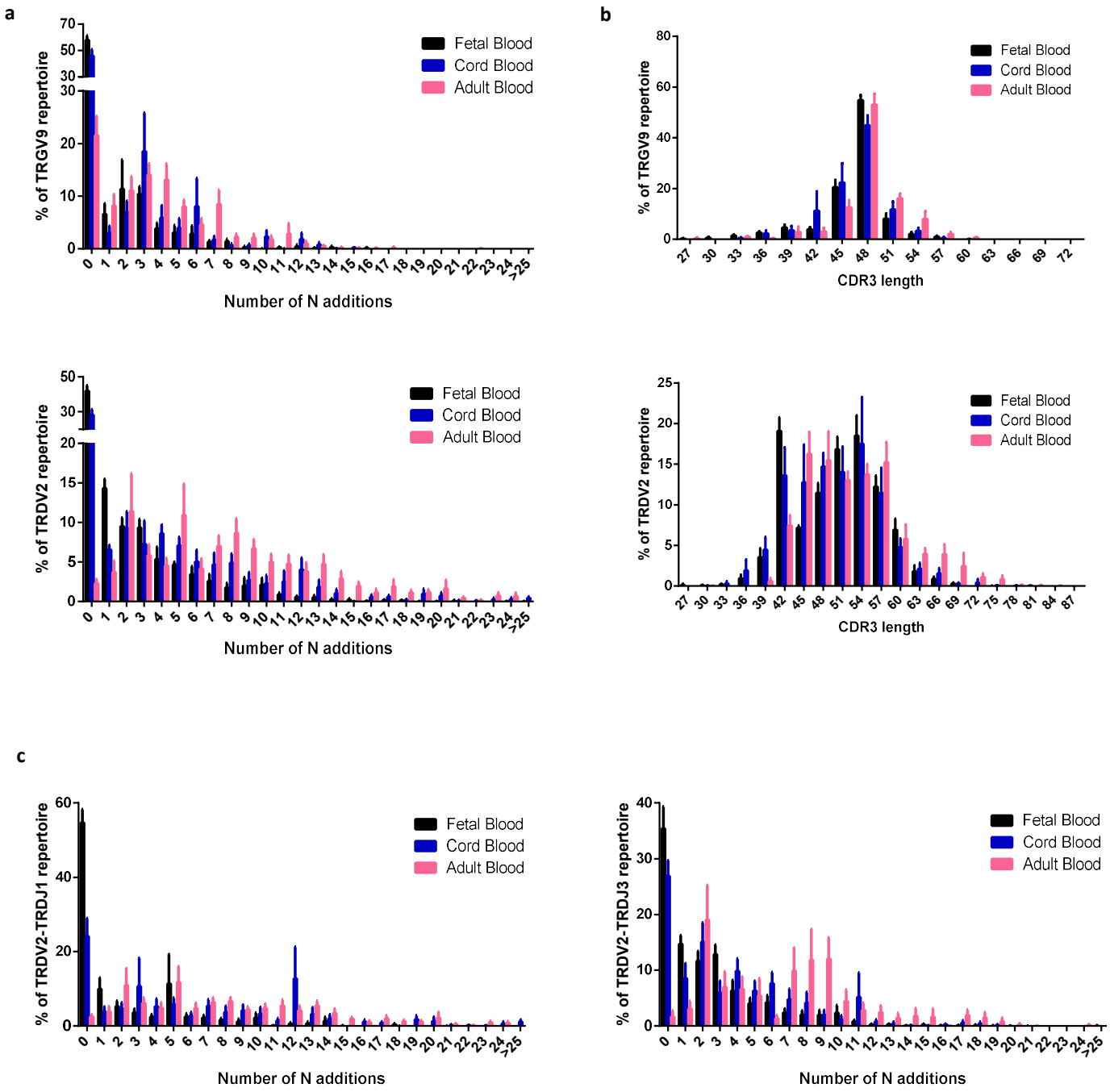

Supplementary Figure 1. CDR3 repertoire of fetal, cord and adult blood Vγ9Vδ2 T cells. a Frequency of TRGV9 (top) and TRDV2 (bottom) CDR3 repertoire per number of N additions. **b** Frequency of TRGV9 (top) and TRDV2 (bottom) CDR3 repertoire per CDR3 length (nucleotide count including the C-start and F-end of the clonotypes). **c** Frequency of the TRDV2-TRDJ1 (left) and TRDV2-TRDJ3 (right) CDR3 repertoire per number of N additions. Data shown from independent subjects, sorted Vγ9Vδ2 T cells from fetal (n=5), cord (n=6) and adult (n=8) blood. Error bars indicate means ± SEM.

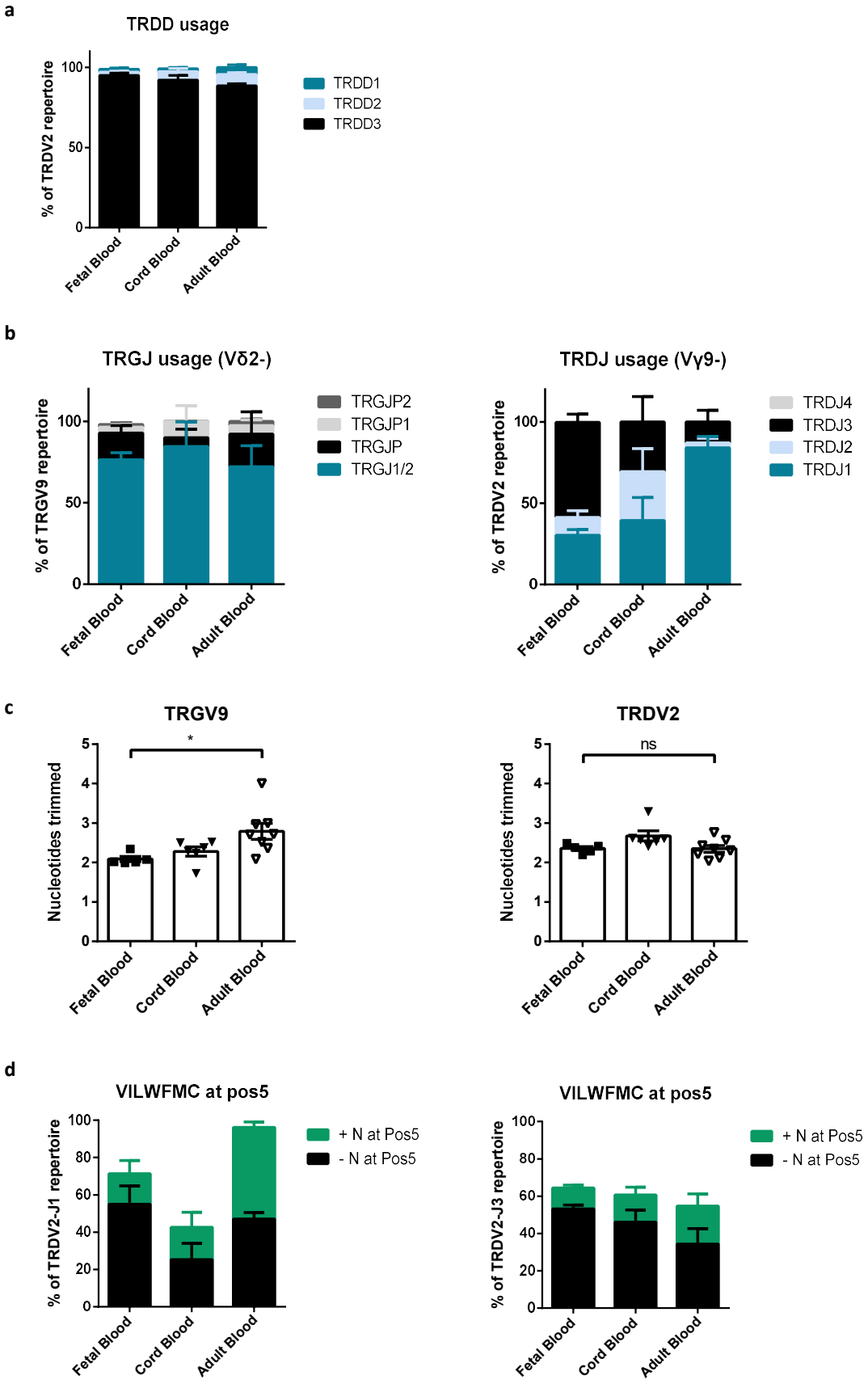

Supplementary Figure 2. CDR3 repertoire of fetal, cord and adult blood γδ T cells. a TRDD usage distribution of the TRDV2 repertoire of sorted Vγ9Vδ2 T cells. **b** J usage distribution of the TRGV9 (left) and TRDV2 (right) of sorted γδ T cells nonVγ9Vδ2 (fetal blood n=4, cord blood n=5, adult blood n=6). **c** Number of nucleotides trimmed at the Vend of the CDR3 of the TRGV9 (left) and TRDV2 (right) repertoire; each dot represents the weighted mean of an individual sample. **d** Percentage of the TRDV2-TRDJ1 (left) and TRDV2-TRDJ3 (right) repertoire containing at position 5 of the CDR3δ a highly hydrophobic residue (V, I, L, W, F, M or C): residue encoded without N additions in black or encoded by N addition(s) in green, of sorted Vγ9Vδ2 T cells. (Sorted Vγ9Vδ2 T cells in a, c and d: Fetal Blood n=5, Cord Blood n=6, Adult Blood n=8.) Error bars indicate means ± SEM. *$p < 0.05$; ns: non significant.

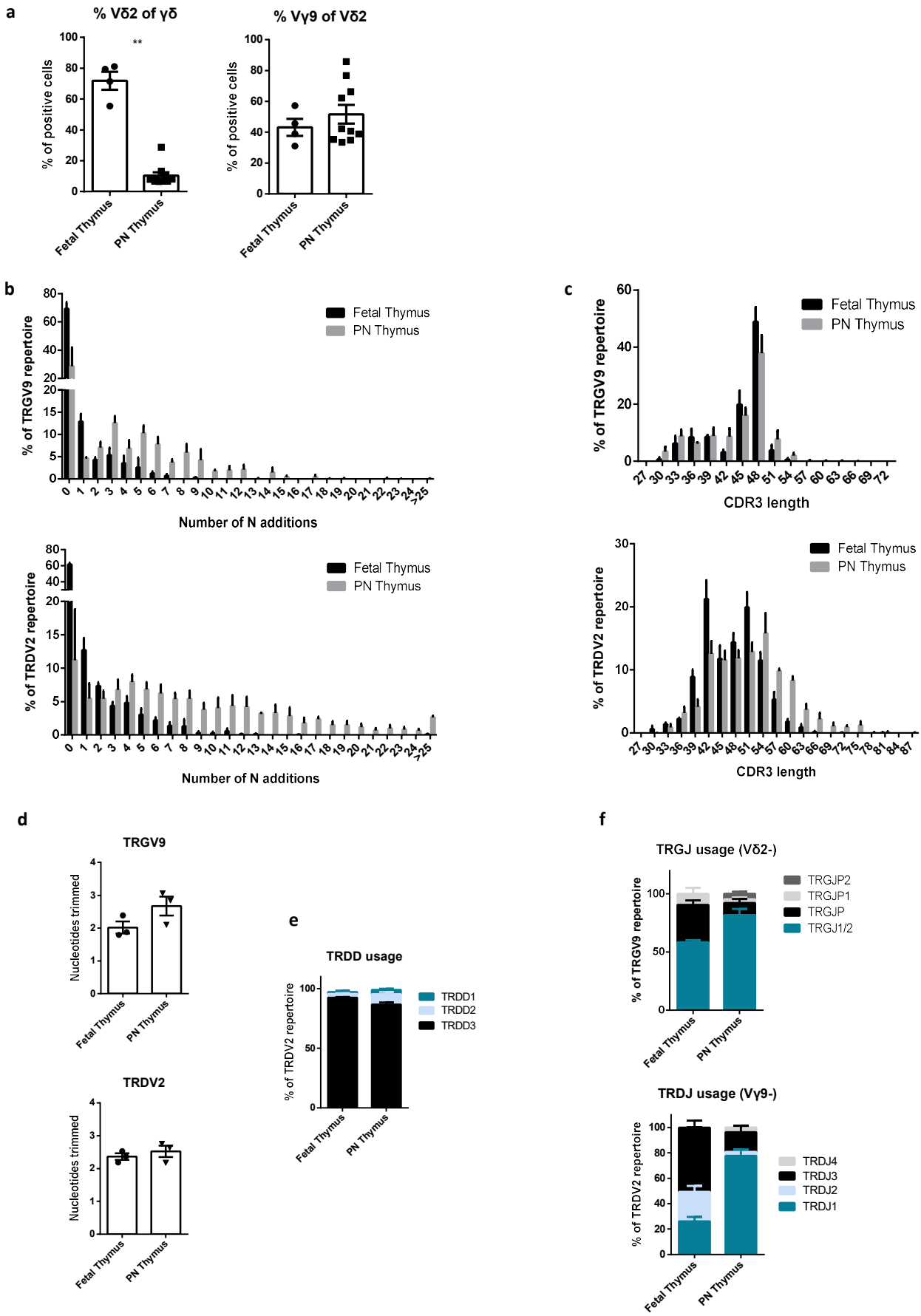

Supplementary Figure 3. Fetal versus post-natal thymus. a Flow cytometry results on the prevalence of Vδ2 of γδ+ (left) and Vγ9 of Vδ2+ (right) thymocytes in fetal (n=4) and post-natal (n=10) thymus. **b-e** Comparison of the CDR3 TRGV9 (top) and TRDV2 (bottom) repertoire of sorted fetal (n=3) and post-natal (n=3) Vγ9Vδ2 thymocytes: **b** Frequency of CDR3 repertoire per number of N additions, **c** Frequency of repertoire per CDR3 length, **d** Number of nucleotides trimmed at the Vend of the CDR3; each dot represents the weighted mean of an individual sample, **e** TRDD usage distribution. **f** TRGJ usage distribution in TRGV9 (top) and TRDV2 (bottom) CDR3 repertoire of sorted nonVγ9Vδ2 γδ+ thymocytes in fetal (n=3) and post-natal (PN) (n=3) thymus. Error bars indicate means ± SEM. **p < 0.01